

CURE MONITORING OF COMPOSITE MATERIALS USING OPTICAL TECHNIQUES

A Thesis submitted
By

Selvarajah Sathiyakumar B.Sc. (Hons), Grad. Dip. (Ed)

For the degree of

Master of Science (Research)

**Optical Technology Research Laboratory
Victoria University
2006**

Declaration

“I, Selvarajah Sathiyakumar, declare that the Master by Research thesis entitled **Cure monitoring of composite materials using optical techniques** is no more than 60,000 words in length, exclusive of tables, figures, appendices, references and footnotes. This thesis contains no material that has been submitted previously, in whole or in part, for the award of any other academic degree or diploma. Except where otherwise indicated, this thesis is my own work”.

Selvarajah Sathiyakumar

Dated the 30th August 2006.

Acknowledgement

I wish to express my sincere appreciation to Prof. Stephen Collins for supervising my Masters research. He gave me frequent advice and criticism and was the major inspiration for this project.

I would like to thank all academic, technical and administrative staff and fellow research students from Applied Physics section (VU) for their kind help and assistance.

I am grateful to my uncle Mr V Packiyasothy and his family for providing accommodation and financial assistance during the periods 1997 – 2000. I also wish to acknowledge my thanks to my family for their love, support and encouragement from start to finish.

Abstract

A fully remote all optical technique for the generation and detection of ultrasonics in epoxy materials has been developed at Victoria University. This requires a high power pulsed laser to induce ultrasound in the sample and an optical fibre interferometer for detection. The output of the interferometer can be recorded using a digital storage oscilloscope and subsequently processed by a personal computer.

This Thesis presents the use of this arrangement for further studies of cure monitoring of composite materials. Samples of 3.0 cm diameter and 1, 2, 4, 6, 8, 10 and 12 cm thickness were made and the interferometer waveforms were recorded in 10 min time intervals after the curing agent was mixed with the epoxy. Attenuation coefficients and travel times were calculated for each waveform.

During the analysis phase of this research an algorithm was developed to find the exact onset of ultrasonic signals. Different thickness samples were made and the interferometric waveforms were obtained and analysed. The relative travel time and wave attenuations were calculated and close correlations were found between these two factors and the state of cure.

In this work, optically-generated ultrasonic waves, when reflecting from the rear surface of an object under test, cause a small surface motion (typically in the range of one tenth of a nanometre to few nanometres). A second diagnostic laser is used to illuminate the rear surface of the test object. The ultrasonic surface motion produces a small phase shift or frequency shift in the reflected light, which is detected by an interferometric system. Signals from the interferometer were recorded using a digital storage oscilloscope (Tektronix DSA 602) and this stored signal is subsequently read and processed using a personal computer. In these experiments, epoxy was poured into moulds and measurements were taken every few minutes thereafter.

Table of Contents

	<i>Page</i>
<i>Declaration</i>	I
<i>Acknowledgment</i>	II
<i>Abstract</i>	III
<i>Table of Contents</i>	IV
<i>Chapter 1 Introduction</i>	
1.1 Introduction	1.2
1.2 Aim of this thesis	1.3
1.3 An Overview of this thesis	1.4
<i>Chapter 2 Background Theory and Literature Review</i>	
2.0 Introduction	2.2
2.1 Laser Irradiation	2.2
2.1.1 Introduction	2.2
2.1.2 Absorption of Electromagnetic Radiation in Metals	2.3
2.1.3 Acoustic Wave Generation and Propagation Mechanism	2.5
2.1.3.1 Thermoelastic effect	2.6
2.1.3.2 Ablation effect	2.11
2.1.3.3 Ablation waveforms at epicentre	2.12

2.2	Practical considerations in laser ultrasonic generation and detection	2.14
2.3	Composite Materials	2.16
2.3.1	Introduction	2.16
2.3.2	Brief History	2.17
2.3.3	Matrices	2.17
2.3.4	Epoxy Resins	2.18
2.4	Non-Ultrasonic Cure Monitoring Approaches	2.19
2.5	Ultrasonic Cure Monitoring Approaches	2.21
2.5	Conclusion	2.26

Chapter 3 Experimental Arrangement

3.1	Introduction	3.2
3.2	Nd: YAG laser	3.3
3.3	Reusable epoxy holder	3.3
3.4	Optical and positioning equipment	3.4
3.5	Acoustic vibration detection system	3.5
3.5.1	Homodyne fibre optic interferometer	3.6
3.5.2	The electronic circuits	3.8
3.5.3	Calibration and characteristics of interferometer	3.10
3.6	Conclusion	3.11

Chapter 4 Results and Discussions

4.1	Introduction	4.2
4.2	Initial results for 1 mm epoxy sample	4.2
4.3	Time delay measurement algorithm	4.9
4.4	Variation of curing time with different thickness samples	4.12
4.5	Variation of time delay with thickness	4.19
4.6	Variation of attenuation with thickness	4.22
4.7	Conclusion	4.24

Chapter 5 Conclusion 5.1

References R-1

List of Publications P-1

Chapter 1

Introduction

- 1.1 Introduction**
- 1.2 Aim of this research**
- 1.3 An overview of this thesis**

1.1 Introduction

The use of composite materials has increased steadily during the past two decades particularly in aerospace, underwater and automotive structures. This is largely because many composite materials exhibit a high strength-to-weight ratio and a high stiffness-to-weight ratio, which make them ideally suited for use in weight-sensitive structures. In addition, many of these materials are more corrosion resistant and more thermally stable than metals. The many advantages of composite materials will enable them to play an even larger role in future generations of military and transportation vehicles as well as in recreational, athletic and medical equipment and numerous other applications in aerospace engineering. The control and monitoring of the curing of these materials is essential. Accurate and active control of composite processing has been recognised as an objective of current research in the processing area. If an active control system is to be designed, there is a need for an on-line, non-destructive cure monitoring technique. These cure-monitoring techniques must be on-line to provide the needed real time feedback of the cure state of the material. It is desirable that they be non-destructive if they are to be used in manufacturing production lines.

In this project cure monitoring using optical techniques was investigated. This involves laser-induced ultrasonics and their detection by a fibre optic interferometer.

1.2 Aim of this research

The aim of this work is to extend the work of Mitra (1997). He demonstrated that using a non contact laser induced ultrasonics method the curing of composite materials can be monitored. In this research:

- i. The remote optical fiber system was reconstructed, aligned and calibrated.
- ii. A reusable epoxy holder was designed and constructed, thereby enabling the use of different thicknesses of epoxy samples during the process.
- iii. An algorithm was developed in Microsoft Excel to analyse the data and find the exact travel time through different thicknesses of epoxy samples.
- iv. The suitability of the non-contact technique for monitoring the curing of composite materials was investigated.

1.3 An overview of this thesis

Chapter 2 describes the principles underlying the laser generation of ultrasonics. The first section deals with absorption of electromagnetic radiations in metals. The principles and the mechanisms involved in the generation of ultrasonics in the thermoelastic and ablation regimes using high power laser are described in next sections. This is followed by practical considerations in laser ultrasonic generation and detection. The section after this briefly reviews the history of composite materials and its significance in modern industrial applications. Chapter 2 also reviews previous work on cure monitoring techniques.

The experimental arrangements are described in Chapter 3. The descriptions about the Nd:YAG laser used was addressed first followed by the complete design details about the epoxy holder and optical arrangements. The section after this is concerns the optical vibration system, and in this section the details about homodyne fibre optic interferometry and the associated electronics are detailed. Chapter 3 concludes with the details about calibrating the interferometer with a vector voltmeter.

Chapter 4 concerns the experimental results obtained using laser generation and remote a fibre interferometer. The chapter also presents the acoustic waveform captured for different thickness samples and the variation of attenuation of acoustics wave as the cure progress. Finally chapter 5 summarises the findings of this research.

Chapter 2

Background theory and literature review

2.0 Introduction

2.1 Laser ultrasonics

2.1.1 Introduction

2.1.2 Absorption of electromagnetic radiation in metals

2.1.3 Acoustic wave generation and propagation mechanism

2.1.3.1 Thermoelastic effect

2.1.3.2 Ablation effect

2.1.3.3 Ablation waveforms at epicentre

2.2 Practical considerations in laser ultrasonic generation and detection

2.3 Composite materials

2.3.1 Introduction

2.3.2 Brief history

2.3.3 Matrices

2.3.4 Epoxy resins

2.4 Non-ultrasonic cure monitoring approaches

2.5 Ultrasonic cure monitoring approaches

2.6 Conclusion

2.0 Introduction

The opening section of this chapter describes the principles and the mechanisms involved in the generation of ultrasonics in the thermoelastic and ablation regimes using a laser. This followed by the practical consideration of laser ultrasonic generation and detection. This chapter also giving a brief history of composite materials and the properties of epoxy resins. The final two sections review previous work on non-ultrasonic and ultrasonic cure monitoring approaches.

2.1 Laser ultrasonics

2.1.1 Introduction

Ultrasonics is broadly recognised to be a powerful non-invasive diagnostic technique. Everyone is familiar with its use in the medical field, particularly to observe a fetus in the womb of the mother. Its use for imaging through opaque materials, particularly to find flowlike cracks, disbounds or delamination is also well known (Blouin *et al.* 1998)

Making a piezoelectric ceramic transducer to vibrate under an electric impulse is the usual method for producing ultrasonic waves. When a low power laser beam strikes a solid surface, some of the incident energy is reflected and the rest is absorbed and converted into heat. The fast temperature rise localised near the surface produces an elastic stress field due to the thermal expansion of the material which, if it remains in an elastic state, constitutes the thermoelastic source. These transient stresses give birth to

acoustic shear, and surface waves whose magnitudes depend on the stimulation regime, thermoelastic or ablation, and the material thermal and optical characteristics.

2.1.2 Absorption of electromagnetic radiation in metals

When a laser beam is incident on a solid surface, in general some of the energy is absorbed by various mechanisms, depending upon the nature of the radiation, while the remainder is reflected or scattered from the surface. We assume that the intensity of the radiation is too low for ablation or some damage process to occur.

The laser radiation that is incident on an absorbing, non-reflecting sample is attenuated as it penetrates the sample. Assuming plane wave propagation in the z-direction, the fraction absorbed δI in any infinitesimal element is proportional to both intensity and the thickness of the element δz , (Scruby 1990) i.e.

$$\delta I = \gamma I \delta z, \quad (2.1)$$

where γ is the absorption coefficient. Then by integration,

$$I(z) = I(0)e^{-\gamma z}, \quad (2.2)$$

which is an exponential form of absorption. However some of the incident radiation will be reflected from the surface, so that

$$I = I' + I'', \quad (2.3)$$

where I' is the absorbed intensity and I'' the reflected intensity, so the reflectivity is given by

$$R = \frac{I''}{I}. \quad (2.4)$$

When the electromagnetic radiation is incident at the surface of the metal, the conduction electrons at the surface screen the interior of the metal from the radiation so that the absorption and reflection take place within a surface layer or "skin". A "skin depth" can be defined (denoted by δ), such that the amplitude of the wave falls to 1/e of its initial value over a distance δ . At longer wavelengths using classical electromagnetic theory (Bleaney and Bleaey ,1965) skin depth, δ , is defined by

$$\delta = (\pi\sigma\mu_r\mu_0f)^{-\frac{1}{2}}, \quad (2.5)$$

where σ , μ_r , μ_0 and f are the conductivity, relative permeability, permeability of free space and wave frequency respectively. The skin depth is reduced for shorter wavelengths and it is also increased for electrical conductivity or permeability.

Classical electromagnetic theory also permits the reflectivity of a clean metal surface to be expressed in terms of the skin depth.

$$R = \frac{2 - 2\xi + \xi^2}{2 + 2\xi + \xi^2}, \quad (2.6)$$

where $\xi = \mu_0\sigma c\delta$ and c is the speed of light.

For most metals, and optical frequencies up to those for visible light, $\xi \gg 1$, so that

$$\text{approximately } R = 1 - \frac{4}{\mu_0\sigma c\delta}.$$

Thus it can be seen that the degree of absorption of the laser beam in the metal will depend upon the radiation wavelength, increasing at shorter wavelength. Substituting different theoretical reflectivity values at different wavelengths, Kaye and Laby (1973) showed generation of ultrasound by lasers to be relatively efficient into steel, especially at shorter wavelengths. The reflectivity of copper changes very rapidly with

wavelength. Kaye and Laby (1973) showed visible or ultraviolet wavelengths are best for efficient ultrasonic generation in copper.

2.1.3 Acoustic wave generation and propagation mechanism

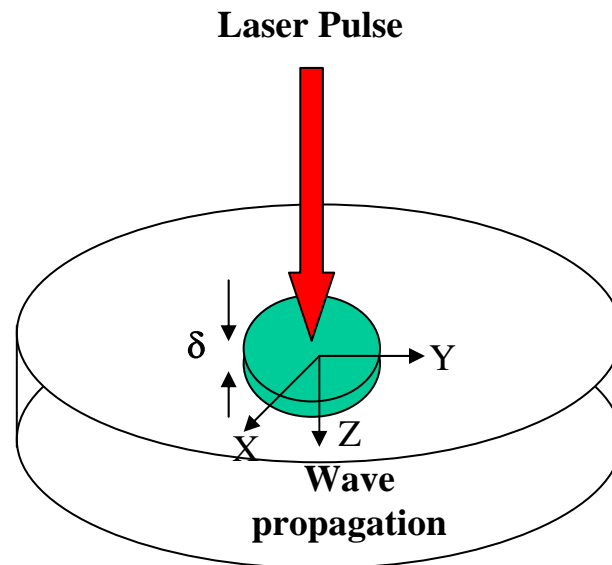


Figure 2.1 Schematic diagram of model for thermoelastic generation of acoustic wave.

When a laser beam is incident on a metal surface, the absorption of radiation normal to the surface is extremely rapid, and normally occurs within the skin depth (δ). As a result of the absorbed radiation energy, a temperature gradient is established within the tiny portion of the metal, which in turn produces a rapidly changing strain field, which radiates energy as elastic waves.

The acoustic wave generation mechanism can be divided into two regimes according to the power density deposited on the metal. A pulsed laser generates acoustic waves through thermal expansion at lower power densities, known as the "thermoelastic

effect", or by vaporizing a small amount of surface material at higher power densities, known as the "ablation effect".

At lower power densities, typically less than 10 MW cm^{-2} , the increase in temperature is sufficiently small to avoid any change of state in the material and the elastic stresses generated are caused by thermal expansion (Scraby 1989). At high power densities, typically greater than 10 MW cm^{-2} , the temperature increase is sufficiently high to cause melting and vaporization at the surface and ejection of a small amount of material.

2.1.3.1 Thermoelastic effect

With an incident laser beam of lower density, the increase in temperature due to the laser pulse is sufficiently small to avoid any change of state in the solid material, and elastic stresses are obtained by bulk thermal expansion. Assume that the absorption of energy δE in a small volume of material V over a time δt causes thermal expansion. The bulk strain is $\delta V/V$. The increase in the volume δV can be given by (Scraby 1990)

$$\delta V = \frac{3\alpha}{\rho s} \delta E \quad , \quad (2.7)$$

where α , ρ and s are the coefficient of linear expansion, density and specific heat respectively.

The instantaneous temperature rise is given by (Scraby 1980)

$$\delta T = \frac{3\alpha}{\rho V \sigma} H(t) \quad , \quad (2.8)$$

where $H(t)$ is the Heaviside step function.

The bulk strain is given by

$$\frac{\delta V}{V} = 3\alpha\delta T. \quad (2.9)$$

Therefore from (2.7),

$$\delta V = \frac{3\alpha}{\rho\sigma} \delta EH(t), \quad (2.10)$$

i.e., the deposition of energy is equivalent to the instantaneous insertion of a small volume of material δV in the metal. Also note that the deposition volume depends only on the total absorbed energy δE and a constant for the material, namely $3\alpha/\rho\sigma$.

For convenience of calculation the effects of wave propagation, δV can be expressed as a sum of three edge dislocation loops, oriented in the three orthogonal directions (Dewhust *et al.* 1982):

$$b_1 A_1 = b_2 A_2 = b_3 A_3 = \frac{1}{3} \delta V, \quad (2.11)$$

where b_i and A_i ($i = 1,2,3$) are the dislocation-loop Burger vectors and areas. Burger vectors gives the direction and size of the lattice deformation that was need to produce the dislocations (Nagel *et al.* 2003).

Since the irradiated volume is at the metal surface, i.e. a normal stress-free boundary, the thermoelastic stress in the z direction is zero, leaving finite x and y stress components.

Now we can calculate the epicentral acoustic displacement at the far side of the metal block. The normal surface displacement at the epicentre U_3 can be given by, (Scraby *et al.* 1980)

$$U_3 = G_{3i,j} D_{ij}, \quad (2.12)$$

where $G_{3i,j}$ and D_{ij} are the Green's function and strength of a force dipole.

A distribution of force dipoles can be related to a distribution of dislocation loops through the elastic constants, C_{ijkl} , i.e.,

$$D_{ij} = C_{ijkl} b_k A_l, \quad (2.13)$$

$$U_3 = G_{3ij} C_{ijkl} b_k A_l, \quad (2.14)$$

From Eq. (2.10),
$$U_3 = G_{3i,j} C_{ijkl} \times \frac{1}{3} \delta V. \quad (2.15)$$

C_{ijkl} can be expressed as

$$C_{ijkl} = \lambda \delta_{ij} \delta_{kl} + \mu (\delta_{ik} \delta_{jl} + \delta_{il} \delta_{jk}), \quad (2.16)$$

where λ and μ are the Lamé constants and δ_{ij} is the Kronecker δ .

Combining equations (2.14) and (2.15),

$$U_3 = G_{3i,j} (\lambda \delta_{ij} + 2\mu \delta_{ik} \delta_{jk}) \times \frac{1}{3} \delta V. \quad (2.17)$$

Hence, U_3 can be written as,

$$U_3 = G^H_{3m,m} (\lambda + \frac{2}{3} \mu) \delta V \quad (2.18)$$

$$= G^H_{3m,m} (\lambda + \frac{2}{3} \mu) (3\alpha / \rho \sigma) \delta E, \quad (2.19)$$

where $G^H_{3m,m}$ is the appropriate Green's function for a Heaviside function source.

Assuming a point source and neglecting thermal conductivity, the computed waveform generated at the epicentre of a plate is shown in Figure 2.2. This simulated waveform predicts an overall depression of the surface at the epicentre. The primary difference between this prediction and the experimental waveform is that the theory does not predict a small positive pulse which is observed at the commencement of the waveform immediately prior to the surface depression.

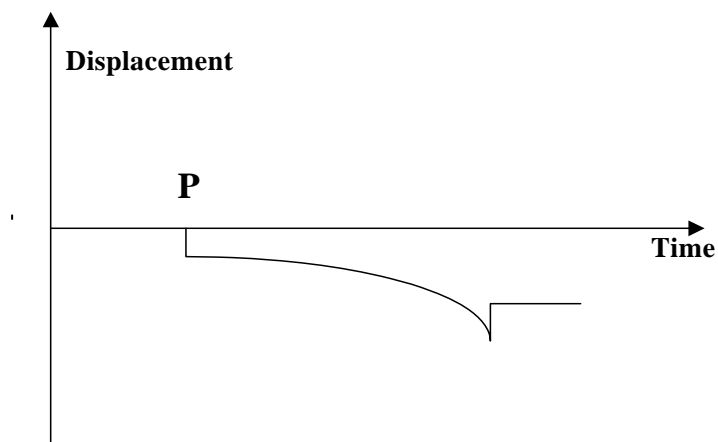


Figure 2.2 Theoretical epicentral waveform calculated excluding thermal conductivity (after Scruby *et al.* 1990).

Taking into consideration the fact that the acoustic source extends over a finite distance into the solid and is not confined to the surface, Doyle (1986) has addressed this problem rigorously and confirmed that the initial spike is indeed due to the effect of thermal diffusion. The theoretical displacement waveform, after considering the effects of thermal diffusion is shown in Figure 2.3.

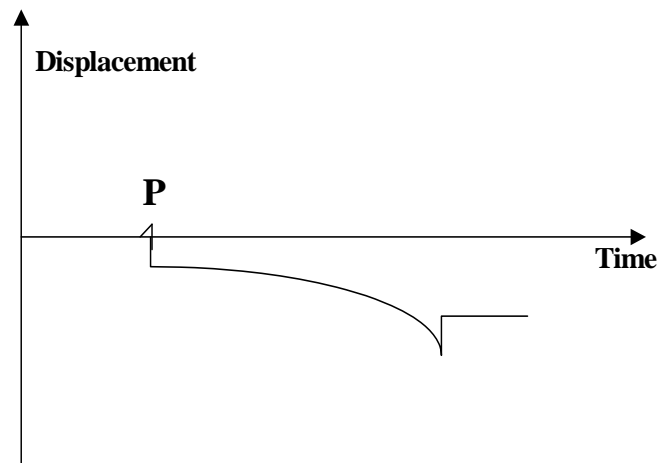


Figure 2.3 Theoretical epicentral waveform calculated including thermal conductivity (after Scruby *et al.* 1990).

The waveform in figure 2.3 clearly shows the initial P-wave pulse, which is absent in figure 2.2, where thermal effects were excluded.

2.1.3.2 Ablation effect

Vaporization of the specimen surface is relatively easy to produce with pulsed lasers. For common metals and typical Q-switched laser pulses it occurs for power densities greater than 10 MWcm^{-2} (Scruby 1989). As the incident optical power increases, the surface temperature rises until the boiling point of the material is reached, and some material is vaporized, ionized and a spark or plasma is formed.

Plasma is formed above the material surface due to the combination of ablation of surface material and high instantaneous temperature caused by absorption of the laser radiation in the materials. Now we can consider the effect caused by the plasma generation in association with ablation. First the plasma exerts a high pressure on the surface which in turn suppresses vaporization of the material by increasing the boiling point of the material well above its normal value. Secondly, it absorbs light from the laser pulse, acting as a shield to keep at extremely hot temperature. Thirdly, as it expands it produces an impulse reaction on the surface and, fourthly, it radiates some of its heat back on the surface, maintaining its high temperature for some time after the incident laser pulse power has started to fall.

2.1.3.3 Ablation waveforms at epicentre

At high power densities, when ablation take place and a plasma is formed, the ultrasonic waveforms and hence the types of acoustic sources are different from the thermoelastic regime considered in the previous section.

In order to calculate the epicentre waveforms in this regime, ablation can be modelled as point force acting normal to the surface of the specimen. Using similar notation to previous sections, it can be shown that the normal surface displacement, U_3 , generated at the epicentre of a parallel plate, in response to a normal point excitation, $F_3H(t)$, on the other surface is given by (Scruby, 1990)

$$U_3 = G_{33} F_3 . \quad (2.20)$$

At constant laser energy, the acoustic displacement amplitude is largely independent of power density. On increasing the power density to form surface plasmas, the acoustic displacement waveforms changes in shape and amplitude, both being dependent on the laser power density as shown in figure 2.4 (Dewhurst *et al.* 1982).

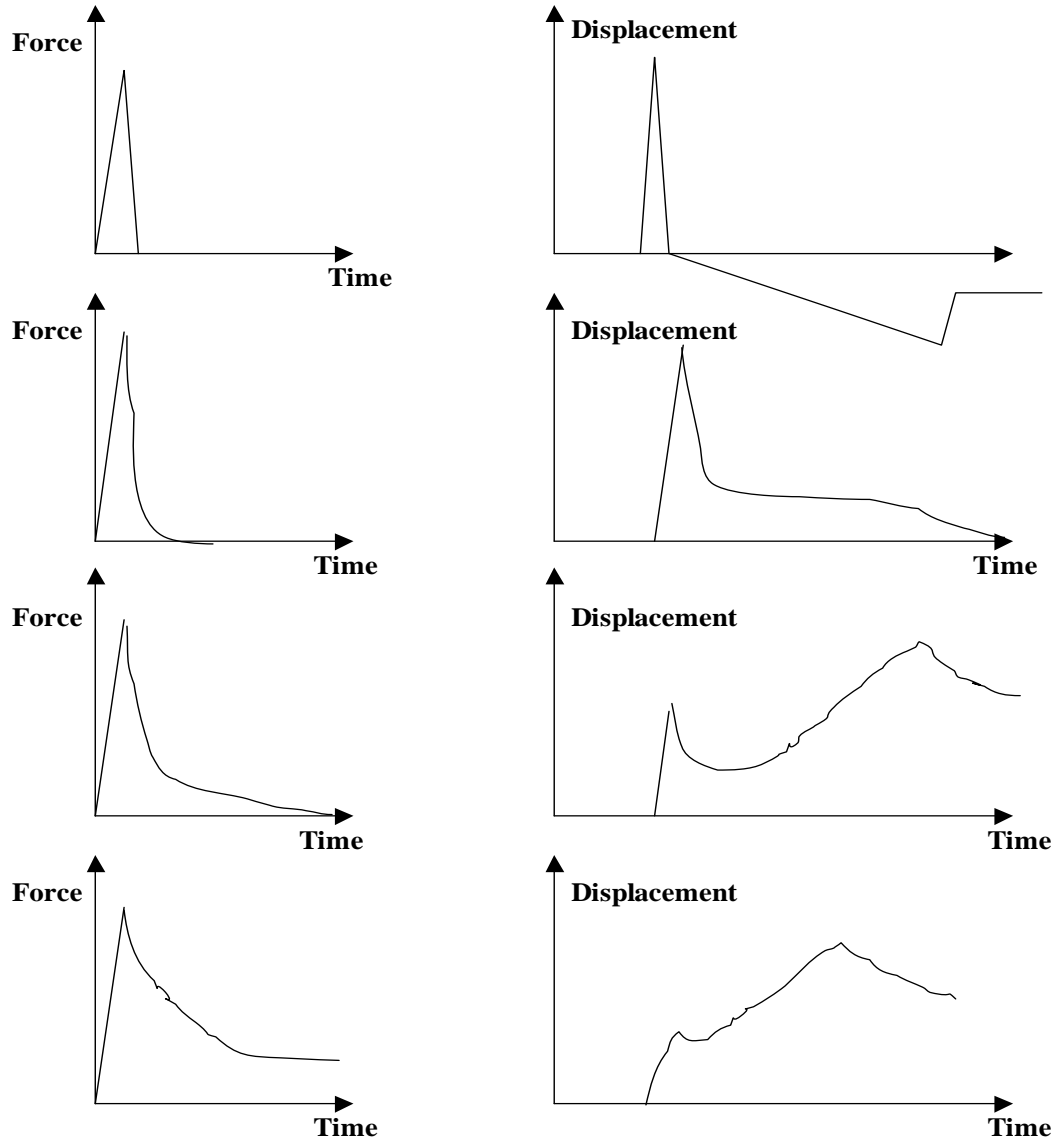


Figure 2.4 Theoretically calculated epicentre waveforms due to high power density ablation for different time domain forces (after Dewhurst *et al.* 1982).

2.2 Practical considerations in laser ultrasonic generation and detection

There are a number of important practical issues that must be appreciated when considering laser ultrasonic generation and detection systems (Scruby 1989).

Advantages over piezoelectric transducers, for both generation and reception, include:

(i) Non-contact: In both generation and reception, there is no physical contact between the laser and the specimen. There is no need for a coupling agent, the electromagnetic radiation couples directly into the surface of the materials, and therefore:

- ◆ No intensity variation or frequency dependent effects due to a coupling layer.
- ◆ The specimen is not affected mechanically by the transducers.
- ◆ The specimen is uncontaminated by the coupling material.

(ii) High spatial resolution: The laser beams used for generation and detection can, in principle, be focused to diffraction limited spots, so that exceptionally high spatial resolution is attainable.

(iii) Good access: One practical consequence of the remote nature of laser ultrasonics, and the small diameter of both the laser beam and the irradiated area of the specimen, is that the technique can be used for applications having limited access. Thus optical fibre can be used to introduce the laser-light to very small, restricted regions of the specimen, where there would be insufficient room for a piezoelectric probe.

However, there also are some drawbacks:

(i) Sensitivity: The ultrasonic amplitudes produced in a metallic specimen by laser generation are comparable with, or slightly smaller than, those generated by a

broadband piezoelectric source. Secondly, the detection sensitivity for ultrasonic displacements using an optical interferometer is no better than that achievable with a piezoelectric transducer.

(ii) Surface finish: Rough or dirty surfaces tends to enhance laser-generated ultrasound, whilst clean, highly polished surfaces are best for interferometric reception sensitivity. Any changes in surface finish will affect the operation of the system.

(iii) Size: Laser systems for generation and reception of ultrasound are generally bulky and heavy. However since optical fibre can transmit light to and from the sample there is little need to have the lasers anywhere near the sample.

2.3 Composite materials

2.3.1 Introduction

Composite materials consist of two or more materials combined to give superior performance to the properties of the individual materials. Although a precise definition for composite materials is not possible, we can understand them according to the following:

- (i) They consist of two or more physically distinct and mechanically separable materials.
- (ii) They can be made by mixing the separate materials in such a way that the diffusion of one material in the other can be controlled to achieve optimum properties.
- (iii) Their properties are superior, and possibly unique in some specific respect, to the properties of the individual components.

There are several types of composite materials available. In this research thermosetting epoxy resins were used. These are isotropic, they don't melt on heating, they have superior strength and elastic properties, a lower shrinkage on curing, and a lower coefficient of thermal expansion.

2.3.2 Brief history of composite materials

One of the earliest recorded examples of a composite can be found in the Bible. It explains the mixing of straw with mud to fashion bricks. The use of concrete, mortar, wood and other ancient composites go back just as far.

Advanced composites arrived on the scene in 1935 with the use of fibreglass filaments in fibre reinforced plastics. Fibre-reinforced plastics were made translucent in the early 50's and were used to make plastic boat hulls, car bodies and trucks cabs. In the late 60's and early 70's, strong aramid, glass and carbon fibres set the stage for the composites in use today (Kathleen *et al.* 1982).

The development of resins began in 1939 with epoxies and in 1969 with phenolics (Kathleen *et al.* 1982). Both types of resins are thermosetting. For the last two decades, boron, silicon carbide and aluminium are joining the ranks of the advanced fibres that endow composites with an extreme modulus of stress.

2.3.4 Matrices

The binding agent in a composite is of critical importance. The four major types of matrices are: polymer, metallic, ceramic and carbon.

Polymer resins are divided broadly into two categories: thermosetting and thermoplastic. In thermosetting polymers, the resin starts as a liquid and is changed to a hard, rigid solid when cross-links are formed at the molecular level. The mechanical properties of the matrices depend on the degree of cross-linking.

2.3.4 Epoxy resins

Epoxy resins have been available commercially for about 45 years and now have many major industrial applications, especially where technical advantages warrant their somewhat higher costs. The technological applications of epoxy resins are very demanding and there are many new developments each year. The term epoxy resin is applied to both the polymer and to the cured resins; the former contains reactive epoxy groups, as illustrated in figure 2.5, and hence their name.



Figure 2.5 The polymer epoxy group

In the cured resins all of the reactive groups may have reacted, so that although they no longer contain epoxy groups the cured resins are still called epoxy resins. The first products that would now be called epoxy resins were synthesised as early as 1891. It was not until the independent work of Castan in Switzerland and Greenlee in the United States that commercial epoxy resins were marketed in the 1940s (Ellis 1993). Although similar resins had been patented in the 1930s the earliest epoxy resins marketed were the reaction product of bisphenol A and epichlorohydrin and this is still the major route for the manufacture of most of the resins marketed today (Ellis 1993).

Epoxy resins find application in areas such as coatings, adhesives or materials for composites. One of the properties required for these applications is that the material should be essentially a rigid solid at the use temperature. In order to convert an epoxy resin to hard, infusible thermoset networks it is necessary to use cross-linking agents.

These crosslinkers, hardeners or curing agents, as they are widely known, promote cross-linking or curing of epoxy resins.

2.4 Non-ultrasonic cure monitoring approaches

It should be noted that various non-ultrasonic approaches have been proposed and developed for cure monitoring of composite materials. Daly *et al.* (1993) used thermally stimulated discharge measurements for the investigation of cure. An epoxy sample was placed in between two circular shape electrodes, in a parallel plate configuration. The electric field, typically of the order of 500 Vcm^{-1} , was applied for different times: 15, 45, 345 and 715 min. After this the sample was cooled to room temperature with liquid nitrogen, whilst the field was maintained. Once cooled down to room temperature the voltage was removed and the sample reheated up to 400 K and the discharge current and temperature were recorded simultaneously. The observed TSD (Thermally Stimulated Discharge) peaks are complex and associated with charge migration coupled with dipolar orientation. These studies show that, whilst the method can be used for monitoring cure, there are problems concerned with the detailed interpretation of the TSD data.

Scott and Patrick (1991) studied the mechanical property development during the cure of an epoxy resin system EPON 815/V140. They used a wide band, 6 MHz transducer to induce ultrasonics. A Panametrics 5052 pulsed receiver was used to excite the transducer with a sharp, broadband pulse. The reflected signal was received with a high frequency (50 MHz) receiver. The signals were displayed on a digital oscilloscope sampling at 100 MHz. The modulus extent, a process parameter for use in

ultrasonic cure monitoring technique, was developed. A comparison was made of the degree of cure as measured by Differential Scanning Calorimeter (DSC), a standard thermal cure characterization technique. In their comparison, the modulus extent shows that significant mechanical property development is still ongoing in the later stages of cure when the degree of cure is fully developed.

Lam *et al.* (1995) monitored the curing of an Epoxy resin EPON 828 using refractive index changes. First, a set of isothermal (60 – 150 °C) cure curves of the epoxy was measured at atmospheric pressure with a Differential Scanning Calorimeter (DSC). The extent of cure as a function of time was found by integrating the heat flow during the reaction and comparing the integrated heat flow to the total heat evolved when the sample undergoes complete cure. Comparison of the extent of cure curves with the refractive index curves yielded the dependence of the refractive index on the extent of cure and temperature. From their studies, they found that within the temperature range 60 – 150 °C the refractive index decreases linearly with increasing temperature. In addition, as the epoxy is cured, the refractive index increases linearly with conversion to the gel point. From then on the shrinkage in volume of the epoxy is restricted by local viscosity. Therefore, the linear relationship between the refractive index and the extent of cure does not hold beyond the gel point.

2.5 Ultrasonic cure monitoring approaches

Thermosetting polymers cure with a chemical reaction that enables the polymer molecules, from both bonds, to create long chains and cross-links between chains. Knowledge of the extent of the bonding reaction during the cure is necessary to optimize the processing of these resins for commercial applications such as resin matrix composites. This knowledge is essential for prevention of over cure or under cure. The rate at which the bonding reaction progresses depends on many variables such as the resin's chemical composition and temperature. Since typically these are not absolutely controllable, a monitor of the extent of cure provides important information useful for controlling the cure process. There are two basic parameters that can be measured with ultrasonic monitors: the time for the wave to transfer through the material (wave speed), and the energy absorbed by the material (attenuation). These parameters can be related to the mechanical response of the materials. It is desirable to relate these parameters to the cure state of the material. For instance, during cure, the wave speed of the composite should increase as the matrix changes from essentially a liquid, to a gel, and finally, to a viscoelastic solid. By monitoring the changes in wave speed and attenuation during cure, the cure state of the material can be assessed.

Winfrey *et al.* (1984) used ultrasonic velocity measurement for cure monitoring. They used a parallel plate glass cell with a 20 MHz broadband transducer bonded to one end of the face of the container. The mixture of curing agent and resin was placed inside the cell and an acoustic wave was propagated through the glass into the resin layer and the resulting echoes from the rear surface of the resin layer were monitored during the curing process. The longitudinal velocity was found to increase monotonically as the elastic moduli of the epoxy increased. The longitudinal velocity was measured for different temperatures and mixtures. The rate of change in the longitudinal velocity with respect to the cure time was shown to vary as predicted by the reaction kinetics, and this demonstrated that the longitudinal velocity was a good measure of the degree of cure.

Hahn (1991) described the ultrasonic characterization of cure monitoring using a piezoelectric transducer to propagate longitudinal waves. Two epoxy systems (Epon 828/2 and Epon 815/v140) were used. The wave speed and attenuation were measured using an ultrasonic flow detector at a frequency of 10 MHz. Three different temperatures were employed; room temperature, 50 and 65 °C. Unfortunately the wave speed didn't vary much with temperature over the range studied.

Scott *et al.* (1991) used ultrasonic and differential scanning calorimeter (DSC) techniques to assess the development of mechanical properties during the cure of an epoxy resin, EPON 815/v140. Five isothermal cures (65, 80, 95, 110 and 125 °C) were ultrasonically monitored with the phase velocity and absorption coefficient being obtained for the calculation of the bulk storage modulus and the modulus extent. The bulk storage modulus and modulus of extent were plotted against cure time and it was found that the bulk modulus increased monotonically until the sample was fully cured. The five isothermal cures were monitored by DSC and compared with the results from ultrasonic methods. In the comparison, the modulus extent showed that significant mechanical property development was still occurring in the later stages of cure when the cure is almost fully developed.

Davis *et al.* (1991) developed a fibre optic Michelson interferometer for the monitoring of a room temperature cured epoxy, Hysel TE6175 epoxy and HD 3561 hardener. The thoroughly mixed epoxy and hardener were poured into a teflon mould. A 600 µm core optical fibre was used to deliver a pulse from a Q-switched Nd:YAG laser to the top surface of the curing specimen. A fibre optic Michelson interferometer was used to detect the arrival of the ultrasonic signal. The sensing arm of this Michelson interferometer was embedded in the curing epoxy specimen. The experiment was designed to measure the variation of time delay between the laser excitation and the arrival of ultrasonic signal as a function of curing time. It was observed that the time delay between the laser excitation and the arrival of the ultrasonic pulse decreased as the cure progressed, thereby showing that the speed of ultrasonic waves increases as an epoxy cures.

Ohn *et al.* (1992) reported an ultrasonic scheme for cure monitoring in room temperature cured epoxy (Hysel EPK 907) and composite (Hercules AS4/1919) using a similar technique to that reported by Davis *et al.* (1991). They employed a pulsed piezoelectric transducer as a source of ultrasound. An embedded interferometric fibre optic sensor, with active homodyne demodulation, was used for the detection of the propagating ultrasonic pulse in epoxies and composites. The sum of the transit times of the longitudinal wave from the source (transducer) to the embedded sensor and the intrinsic electronic system delay, defined as the τ parameter, was measured as a function of the cure time. The τ parameter was found to decrease monotonically as the cure progresses and exhibited the same trend as the change of viscosity during the cure of an epoxy or an epoxy-based composite. This technique provides a satisfactory means of cure monitoring during fabrication.

Dorigi *et al.* (1997) used a complete fibre optic ultrasonic system to monitor the cure of an epoxy resin at room temperature. Ultrasound was generated by using a 1000 μm core fibre to deliver light from a Nd:YAG Q-switched laser to the aluminium mould containing the epoxy. An intrinsic fibre optic Fabry-Perot interferometer was embedded in the epoxy to detect ultrasonics. They also used piezoelectric transducers for ultrasonic generation. Both the ultrasonic attenuation and ultrasonic signal velocity measured using this complete fibre optic ultrasonic systems were consistent with similar measurements performed using a piezoelectric transducer for the generation of ultrasound.

Mitra (1997) used a fully remote all optical technique for the generation and detection of ultrasonics in epoxy materials. A Q-switched Nd:YAG laser operating at a wavelength $1.06 \mu\text{m}$ was used with a pulse length of about 10 ns and a maximum energy of 1300 mJ at the target, which was placed at a distance of 15 cm from the laser. The displacement of the rear target surface on arrival of the ultrasonics was monitored by an optical fibre Michelson interferometer, having its measuring end at a distance of 20 cm behind the rear target surface. He used a fast curing epoxy as the target material (rapid cure ATL composite) and a container of dimension $59 \text{ mm} \times 35 \text{ mm} \times 14.5 \text{ mm}$ (thickness) to hold the liquid epoxy. From his experimental results the relative attenuation drops almost an order of magnitude as the cure progressed and the propagation time also decreases substantially as the cure progressed.

In most of the work reported so far, the longitudinal wave velocity was chosen as a measure of the extent of cure since Hahn (1991) demonstrated a monotonic increase in this velocity as the cure progresses. The change in velocity is related to the extent of cure because the elastic moduli are dependent on the cross-link density in the epoxy and this density increases with cure time (Hahn 1991).

2.6 Conclusion

The ultrasonic cure monitoring is non-destructive technique and can be used to monitor the curing process during fabrication. So far only Mitra (1997) have studied and developed a non-contact experimental arrangement for laser generation and detection. He also demonstrated that the same experimental arrangement can be use for cure monitoring. There have been no works reported on the cure monitoring of different thickness samples by non-contact laser ultrasonic methods. This work is an extension of Mitra (1997) investigation, to find how well the system will work for different thickness epoxy samples.

Chapter 3

Experimental arrangement

3.1 Introduction

3.2 Nd: YAG laser

3.3 Epoxy Holder

3.4 Optical and positioning equipment

3.5 Acoustic vibration detection system

3.5.1 Homodyne fibre optic interferometer

3.5.2 The electronic circuits

3.5.3 Calibration and characteristics of interferometer

3.6 Conclusion

3.1 Introduction

To investigate the curing of composite materials using laser induced ultrasonics and a fibre optic interferometer certain apparatus and procedures were required. This chapter first outlines the major equipment items used, and then the experimental procedures undertaken. The overall experimental arrangement for studying curing of epoxy samples was as shown in figure 3.1. It can be divided into two parts, acoustic vibration excitation and acoustic vibration detection. The acoustic vibration excitation system consists of a Nd:YAG laser and a plano-convex lens and the detection system consists of an all fibre interferometer and a digital signal analyzer.

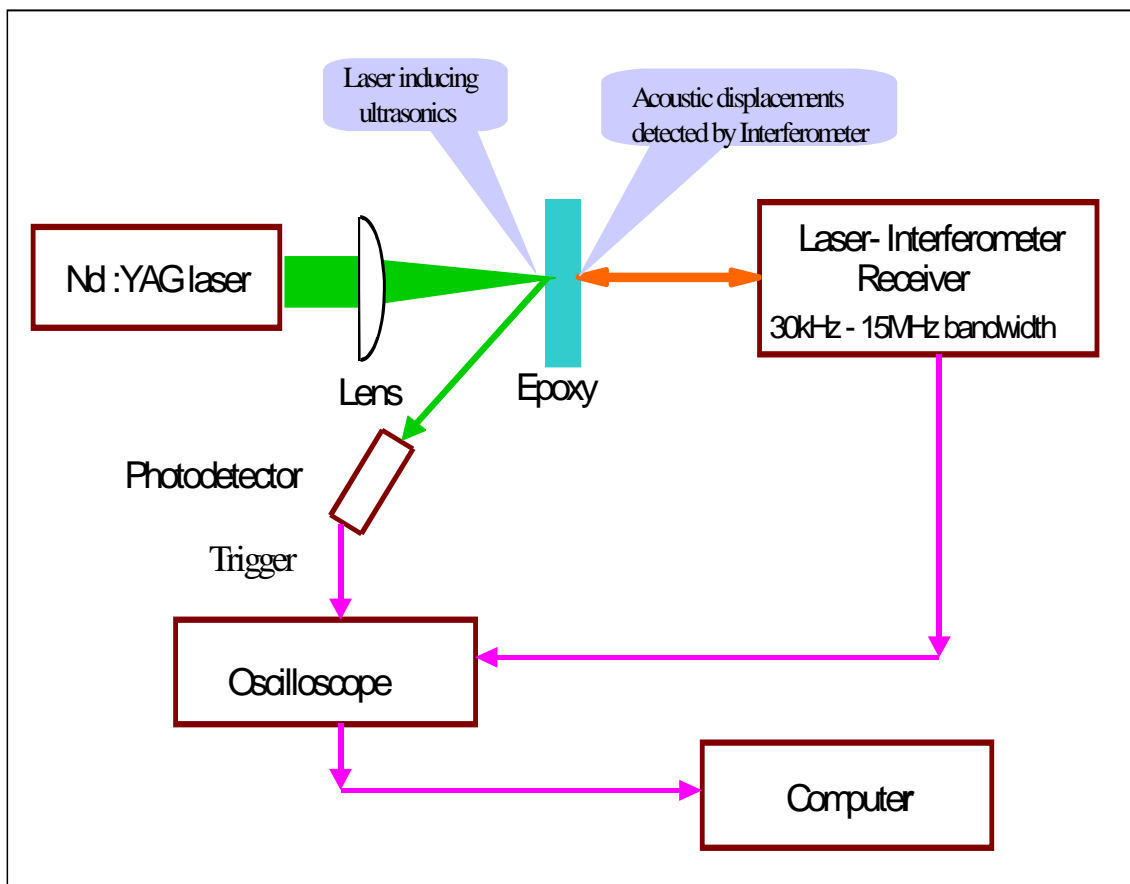


Figure 3.1 Schematic diagram of the experimental arrangement

3.2 Nd:YAG laser

The laser used to induce ultrasonics in non ablation regimes was a Q-switched Nd:YAG laser (Quanta-Ray GCR series, manufactured by Spectra Physics). The laser pulses were triggered by an external switch. The specifications of the laser are listed in table 3.1.

Wavelength	532 nm
Beam Diameter	1 cm
Output Energy	130 mJ/pulse
Pulse width	10 ns

Table 3.1 Specifications of the Spectra Physics Q-switched Nd:YAG Laser

3.3 Reusable epoxy holder

An epoxy holder was constructed using Teflon, as shown in Figure 3.3. The inner diameter of the epoxy holder was 3 cm and the thickness can be varied from 1 mm to 10 cm. Since the epoxy won't stick to the Teflon, the same holder was used for repeated experiments. The epoxy was poured into the container and pressed hard to make a perfect contact with the front and back surfaces. The front side of the holder was a 0.25 mm thickness Teflon disc and the rear side can be replaced with different thickness copper strips. The front surface was painted with silver paint to get good reflection for the interferometer beam back into the sensing fibre tip.

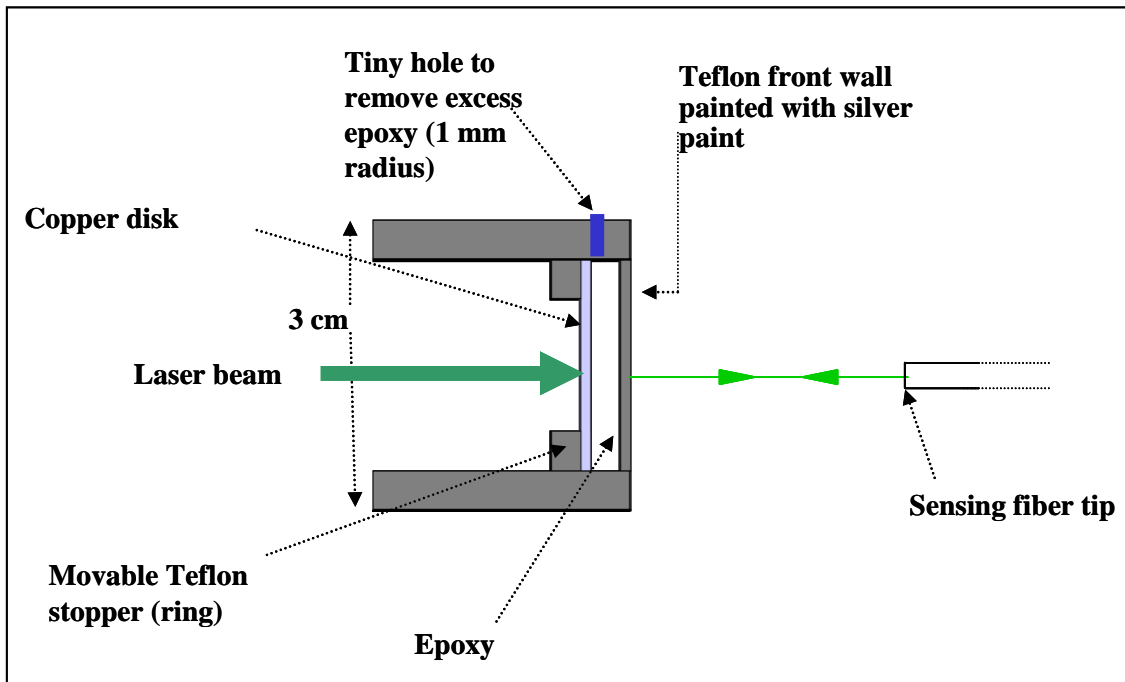


Figure 3.3 Cross sectional view of the epoxy holder

3.4 Optical and positioning equipment

Basic optical equipment was used in most of the experimental work as shown in figure 3.4. A plano-convex lens was used for focusing the 532 nm laser beam. Microscope objective lenses were used in coupling assemblies with mechanical XYZ stages to couple light into fibres. Microscope objectives were used to focus the laser onto the front surface of the epoxy holder and get reflections from it. Optical rails were used to align the optical paths on the optical table.

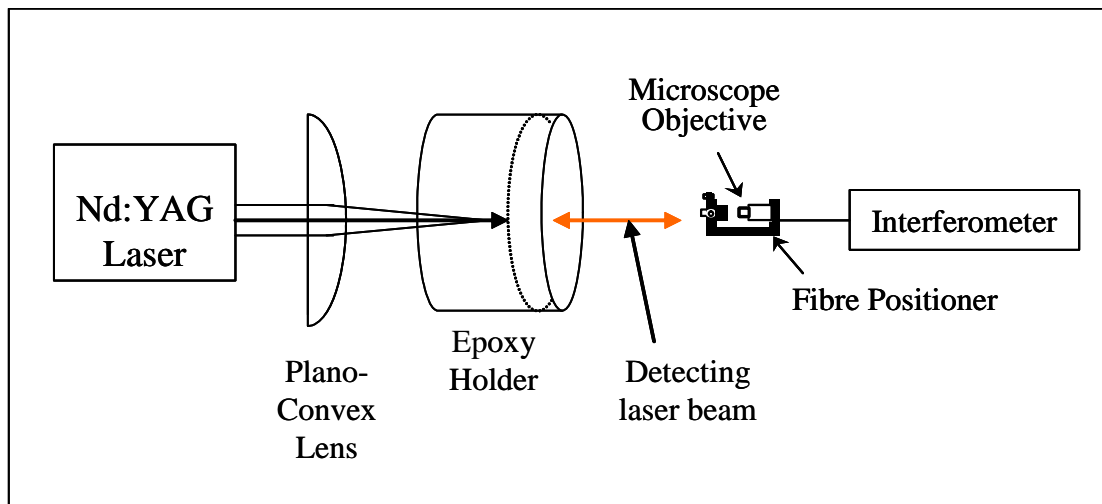


Figure 3.4 Bulk optical arrangement of the experiment

3.5 Acoustic vibration detection system

The acoustic vibration detection system includes the laser source and the all Mach-Zehnder configuration fibre optic interferometer (Figure 3.5) with detection electronics (Figure 3.6). The system was developed and used by Mitra (1997). The detection electronics system converts an optical output to an electrical signal, which after amplification and differentiation is displayed on an oscilloscope (DSA602). All measurements were obtained in the form of displacement response curves, and were stored on disc using an HP-Basic program, which enabled data transfer from the DSA to a computer through a standard GPIB interface.

3.5.1 The homodyne fibre optic interferometer

The experimental arrangement for the homodyne type Mach-Zehnder fibre optic interferometer is shown schematically in Figure 3.5. The light source was a stabilised He-Ne laser (Spectra-Physics 117A), emitting approximately 1.5 mW of light at a wavelength of 632.8 nm. The directional couplers DC1 and DC2 are standard 633 nm devices. In order to obtain high fringe visibility, the optical power in the signal arm is matched approximately to the optical power in the reference arm using an optical attenuator formed by winding a number of small radius turns of fibre in the reference arm. Where possible, the two optical fibres (signal and reference arms) are paired closely together and therefore are largely subjected to the non-signal perturbations and hence the same perturbation-induced phase changes. This tends to minimise thermal drift. The path length of each arm is 300 cm (input DC1 to input DC2). In order to hold the interferometer at the quadrature position, a phase modulator is incorporated in the reference arm of the interferometer. This phase modulator has 30 turns of single mode fibre (Corning Flexcore 633) wound around a piezo-electric cylinder (Tokin XOZ-138) of outside diameter 38 mm, inside diameter 36 mm and height 30 mm. In this arrangement, the number of volt-turns for a 2π radian phase shift with an 18 volt supply provides ample drift compensation range for the interferometer (much more than a 2π radian phase shift). To avoid thermal effects, the directional couplers, attenuator and piezoelectric cylinder were housed in a box made by cutting appropriately-shaped components in a solid block of styrofoam. The channel in which the fibre was placed was made to avoid small radius bends to reduce unwanted signal losses.

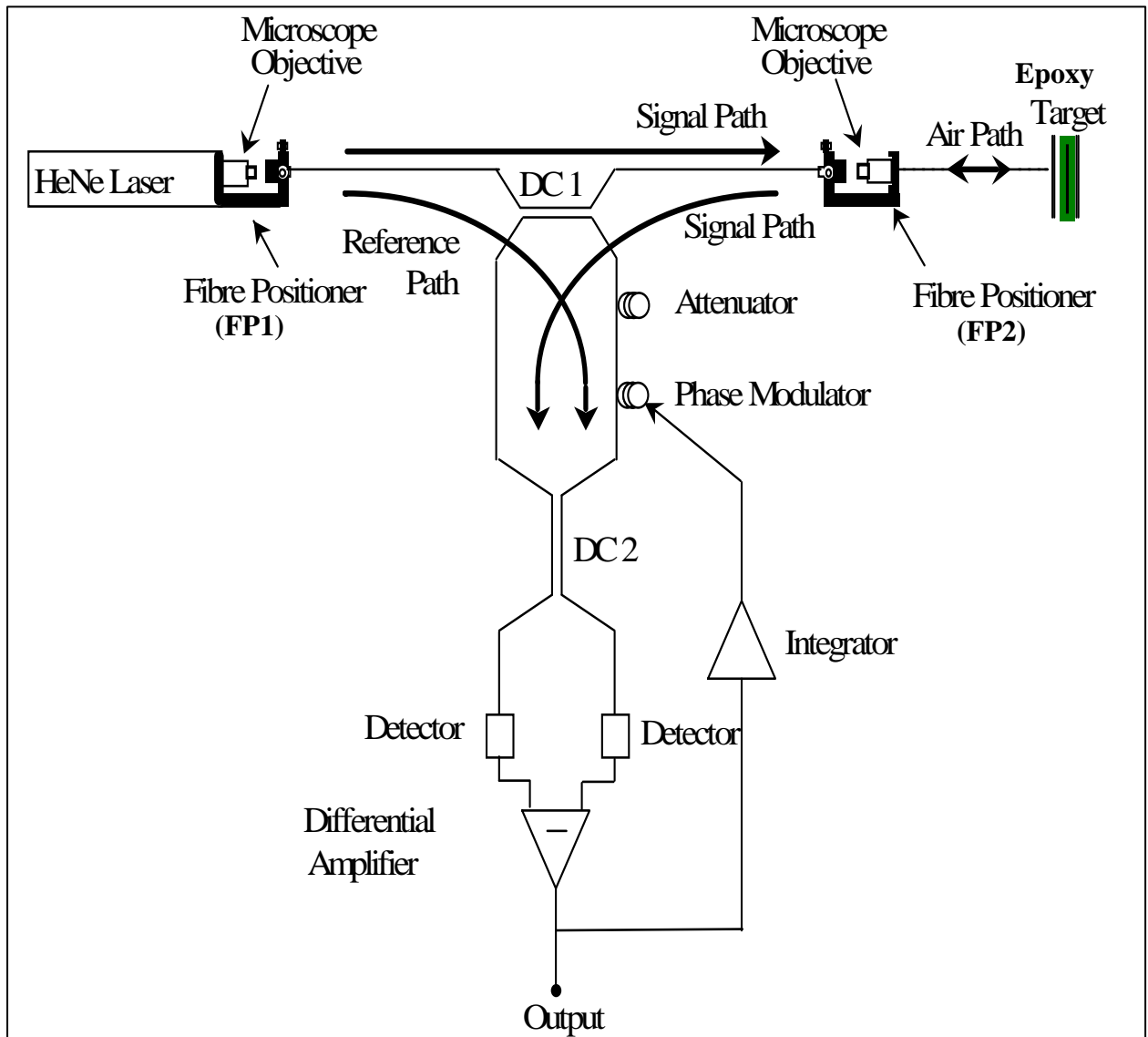


Figure 3.5 Optical layout of the homodyne interferometer (after Mitra 1997).

3.5.2 The electronic Circuits

The circuit diagram for the detector electronics and signal-processing unit is shown in figure 3.6. In this circuit, in order to minimize the common mode noise the subtraction of the currents in the photodiodes (OPF480) is done before amplification. An NE5212 transimpedance amplifier with a bandwidth of 140 MHz was used as the first stage. Two channels were derived from the output of this stage. The first was used to recover the desired signal (the high-frequency channel) and the second was used to give a low frequency and reduced noise output (labelled LF output in the diagram) for use in applications in which the wide bandwidth is not required. The low frequency output was integrated (U6) and a bipolar signal was then generated (U3 and U5) to drive the piezoelectric modulator. The use of a bipolar output extended the locking range obtainable with the interferometer when using low-voltage batteries as the supply. In the high frequency channel, the output of the first stage was high pass filtered and then amplified using another NE5212 as a voltage amplifier. The high frequency signal can be recovered from either of the differential outputs of this second amplifier. To isolate the circuit from the main supply and from the noise generated by the Nd:YAG laser, the circuit was powered by ± 18 V batteries mounted inside the shielded detector box.

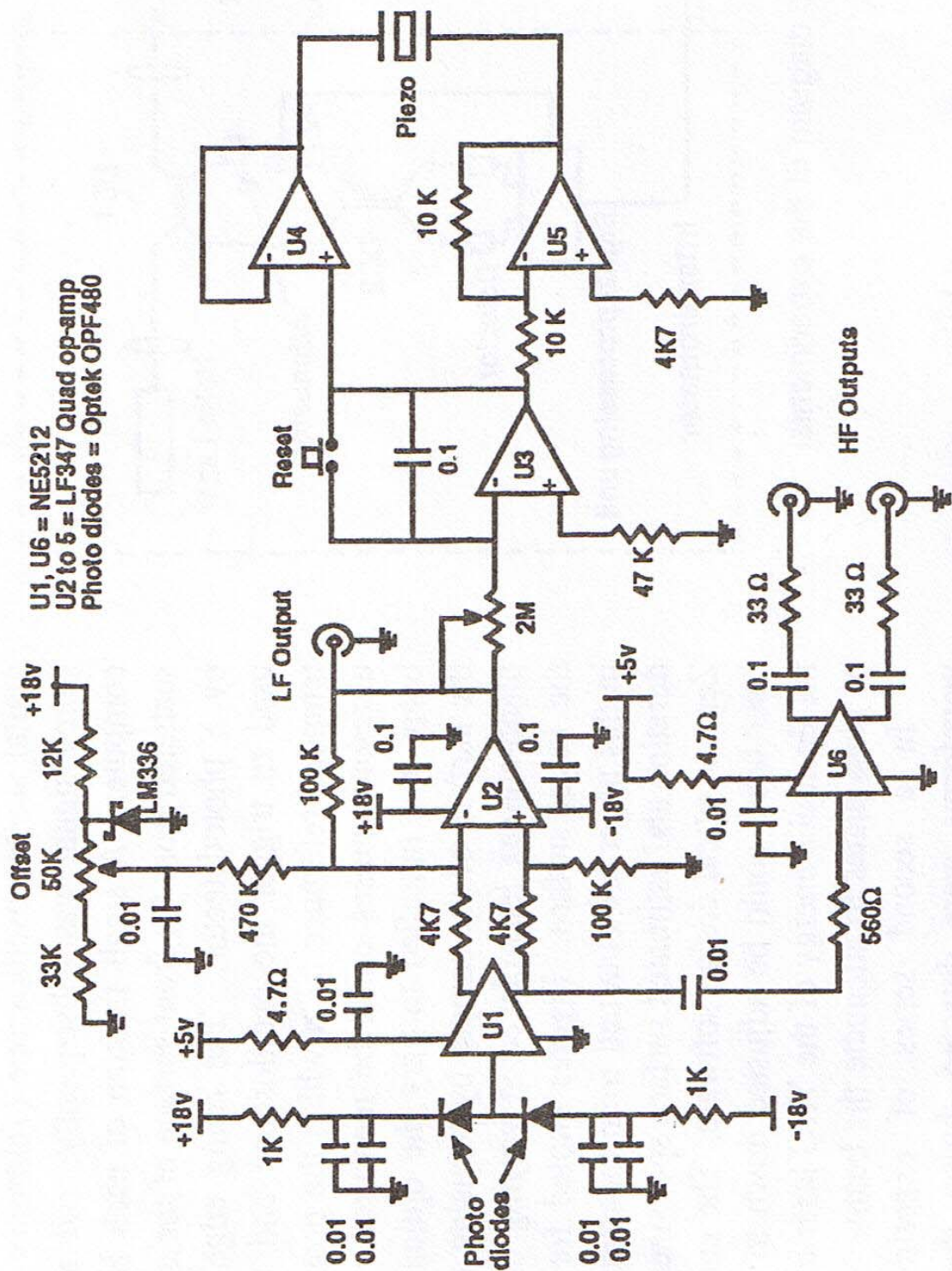


Figure 3.6 Circuit diagram for the detector electronics and signal-processing unit (after Mitra 1997).

3.5.3 Calibration and Performance of Interferometer

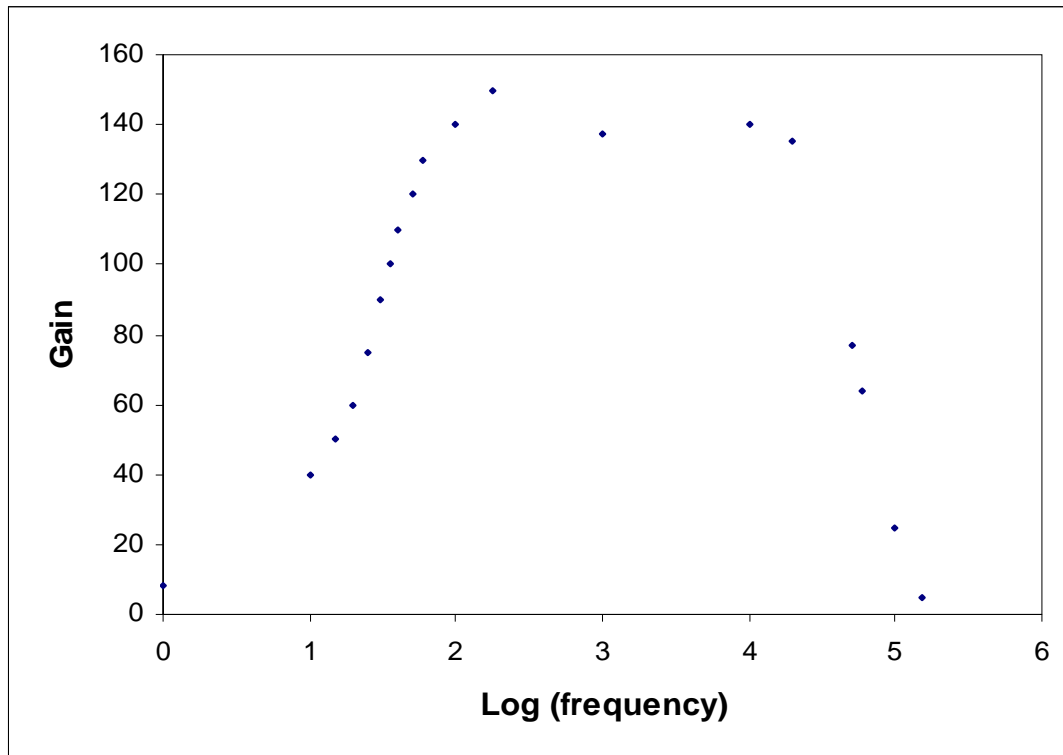


Figure 3.7 Gain ($\frac{V_{out}}{V_{in}}$) vs Log (frequency in Hz) graph for the interferometer

The interferometer was calibrated using a piezoelectric mirror shaker (Mb-ST/500/3). The mirror shaker was mounted on the optical rail replacing the epoxy holder. The frequency of the mirror shaker was changed and reflected light was coupled back into the signal arm of the interferometer. To determine the frequency response of the interferometer a vector voltmeter was used. The gain, determined as a function of frequency and calculated as $\frac{V_{out}}{V_{in}}$, is plotted in Figure 3.7, where the X axis is Log (frequency) with frequency measured in Hz. It can be seen that the interferometer responded to a wide frequency range; a 15 MHz bandwidth was determined for the interferometer.

3.6 Conclusion

The experimental arrangement described in this chapter was used for non contact laser generation and detection of acoustic waves. The Nd:YAG laser is capable of producing ultrasonic waves in the non ablation regime. The transmitted ultrasonic wave vibration can be detected using the 15 MHz bandwidth Mach-Zehnder fibre optic interferometer. The interferometers logging time was 20 sec and the interferometer should be reset before making each measurement. The details about the waveforms measured are provided in the next chapter.

Chapter 4

Results and discussion

4.1 Introduction

4.2 Initial acoustic waveform results for 1 mm epoxy sample

4.3 Time delay measurement algorithm

4.4 Variation of curing time with different thickness samples

4.5 Variation of time delay with thickness

4.6 Variation of attenuation with thickness

4.7 Conclusion

4.1 Introduction

In this chapter the experimental results obtained using the equipment described in the previous chapter are presented. Initially a 1 mm epoxy sample was made and the interferometric waveform was captured and analysed. Later the same procedure was extended to epoxy samples of 2, 4, 6, 8, 10 and 12 mm thickness. An algorithm using Excel software was developed to determine the first ultrasonic pulse arrival time. After that the variation of relative travel times against thickness were calculated. Then the variations of relative ultrasonic attenuation for different thickness of epoxy samples are presented.

4.2 Initial acoustic waveform results for 1 mm epoxy sample

The experimental arrangement, described in Chapter 3, was used to make measurements. The epoxy holder was adjusted to hold a 1 mm thickness sample. The epoxy was mixed with the curing agent in a ratio of 5:1, mixed thoroughly and degassed using a manual vacuum chamber. Once the sample was ready it was poured into the cylindrical-shape epoxy holder of radius 2 cm, as described in section 2.2, and pressed tightly to make perfect contact with the front and back surfaces of the epoxy

holder. The interferometric waveforms were recorded in 5 minute intervals from the start of the curing process.

The recorded interferometric waveforms for a 1 mm sample are shown in figures 4.1. This figure shows all waveforms recorded for a period of 90 minutes after the curing process started. Similar trend is found in all waveforms recorded after 10 min. A small bump of an ultrasonic pulse is arising for the first time around 5.2 μs for the signal which was recorded 15 min after the curing process started. The same bump of pulse was observed in all waveforms recorded thereafter. It is also observed all bump of pulses are arriving in a small time domain. This region was highlighted as first pulse arrival region in figure 4.1. To observe individual properties of the waveform behaviour the graphs were grouped in to four as shown in figure 4.2-4.4. Similar waveforms were reported by Mitra *et al.*, (1996), who used same type of epoxy with a different dimension epoxy holder. Other researchers, Lindrose (1978), Hahn *et al.*, (1984) and Ohn *et al.*, (1992) also reported similar trend waveforms. The time delay between the trigger pulse and the onset arrival of the first ultrasonic pulse is a factor to determine the end of the cure state. The longitudinal velocity can be calculated using the travel time.

The longitudinal wave velocity was chosen as a measure of extent of cure since Hann (1994) had already demonstrated a monochromatic increase in this velocity as the cure progresses. The change in longitudinal velocity is related to the extent of cure because

the elastic moduli is dependent on the crosslink density in the epoxy and this density increases with cure time (Winfrey and Parker, 1984).

Figures 4.1-4.4 clearly indicating that the amplitude of the first arrival pulse is increasing and the time interval between the first pulse and the trigger signal is decreasing. As the cure process started the mechanical properties of the epoxy changed significantly allowing faster ultrasonic propagation. The time interval between the trigger pulses to the onset of the rise of the acoustic pulse is the propagation time. Since the waveforms recorded at early stages of curing were significantly affected by the noise picked up from the electronic circuits the uncertainty in determining the onset of the acoustic pulse is the major source of uncertainty in the propagation time. To overcome this problem the front surface of the epoxy holder was painted with silver paint to get good reflections to improve the signal amplitude.

To determine the onset pulse arrival time, different techniques were tried and finally an algorithm is developed using Excel. The full detail of the algorithm development was described in the next section.

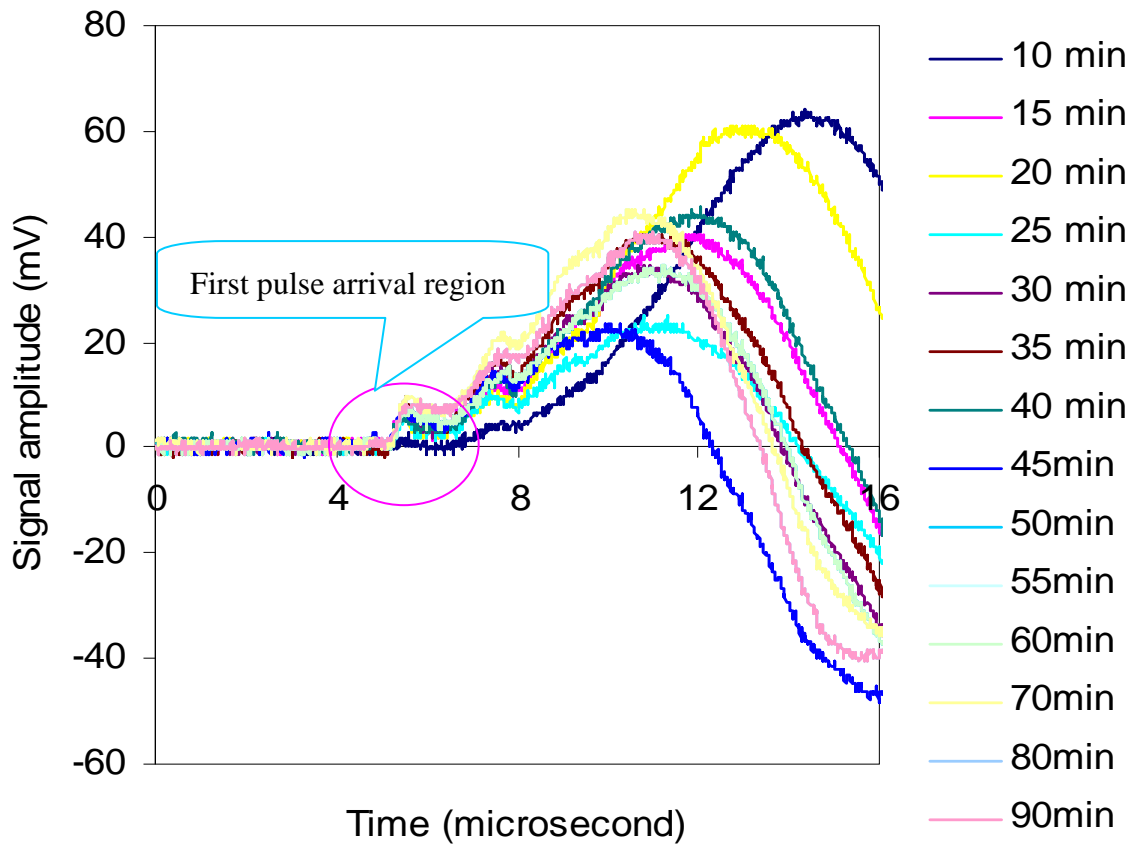


Figure 4.1 Interferometer waveforms for the arrival of an acoustic wave during the early stages of cure in a rapid cure room temperature epoxy. The epoxy holder was adjusted to hold 1 mm thickness of the room temperature cure epoxy. The signals were recorded for the first 90 min after the epoxy was mixed with the curing agent.

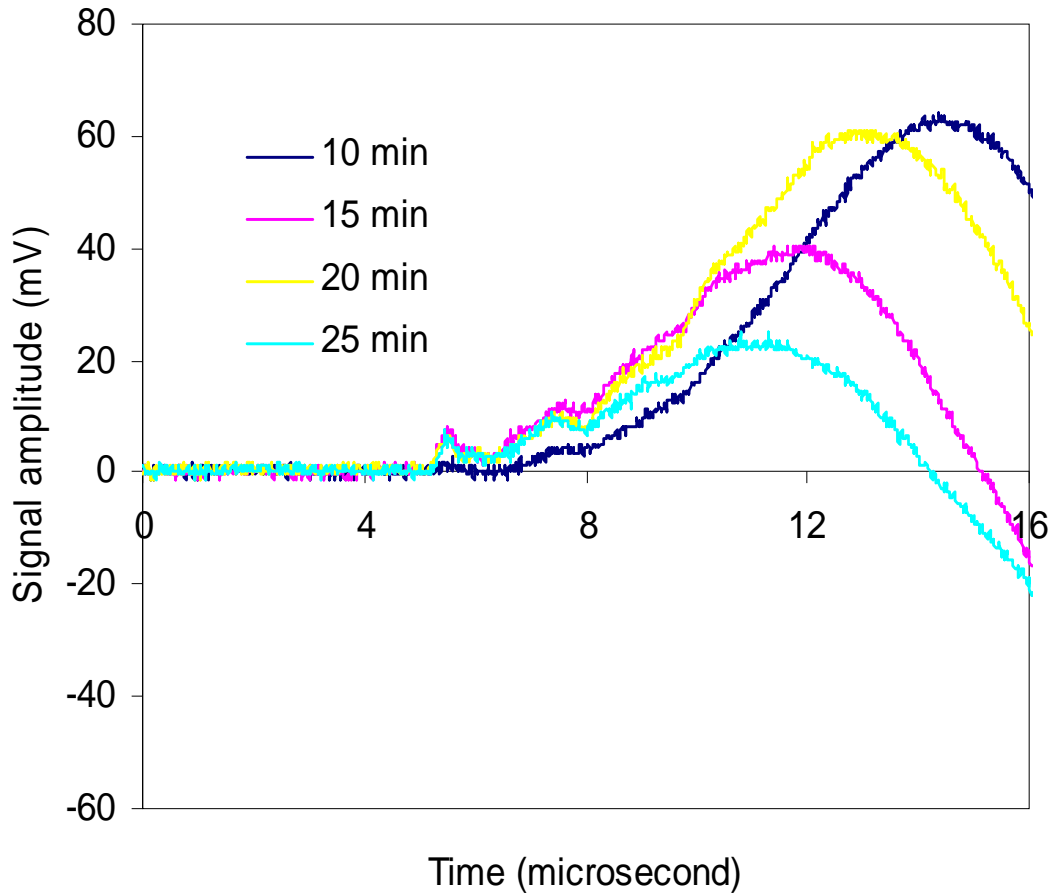


Figure 4.2 Interferometer waveforms for the arrival of an acoustic wave during the early stages of cure in a rapid cure room temperature epoxy of 1 mm thickness at room temperature. The signals were recorded 10, 15, 20 and 25 min after the epoxy was mixed with the curing agent.

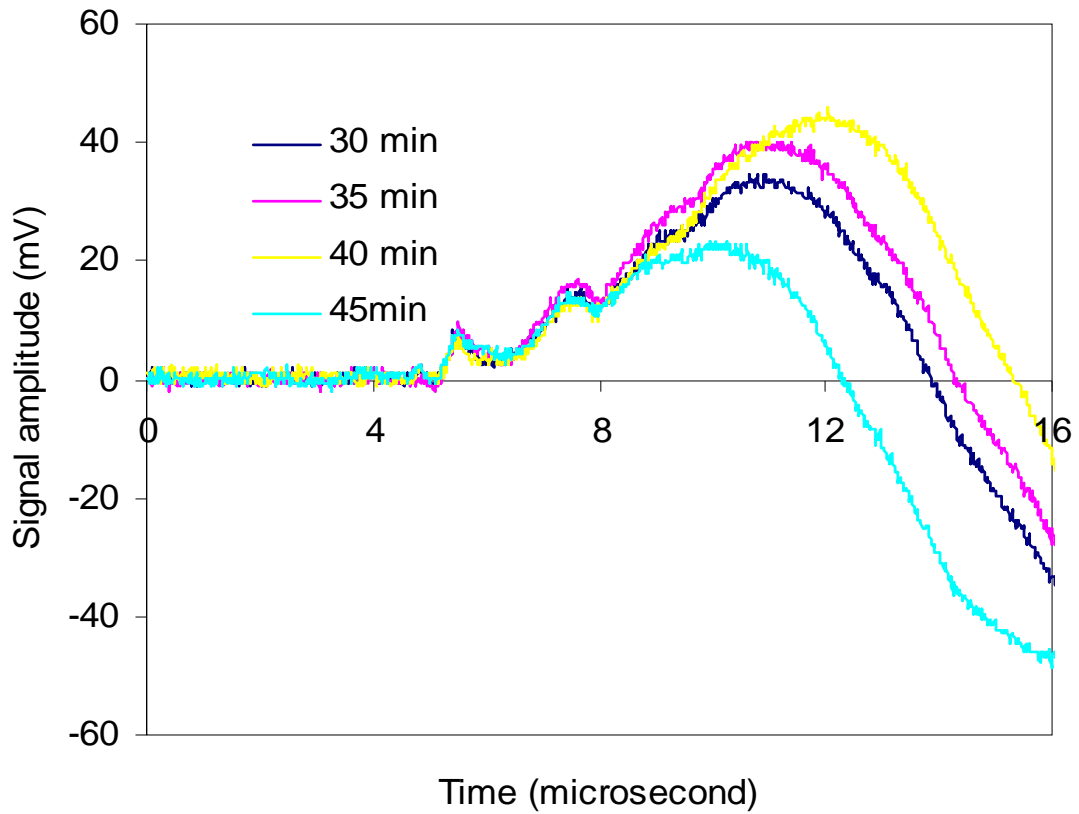


Figure 4.3 Interferometer waveforms for the arrival of an acoustic wave during the early stages of cure in a rapid cure room temperature epoxy of 1 mm thickness at room temperature. The signals were recorded 30, 35, 40 and 45 min after the epoxy was mixed with the curing agent.

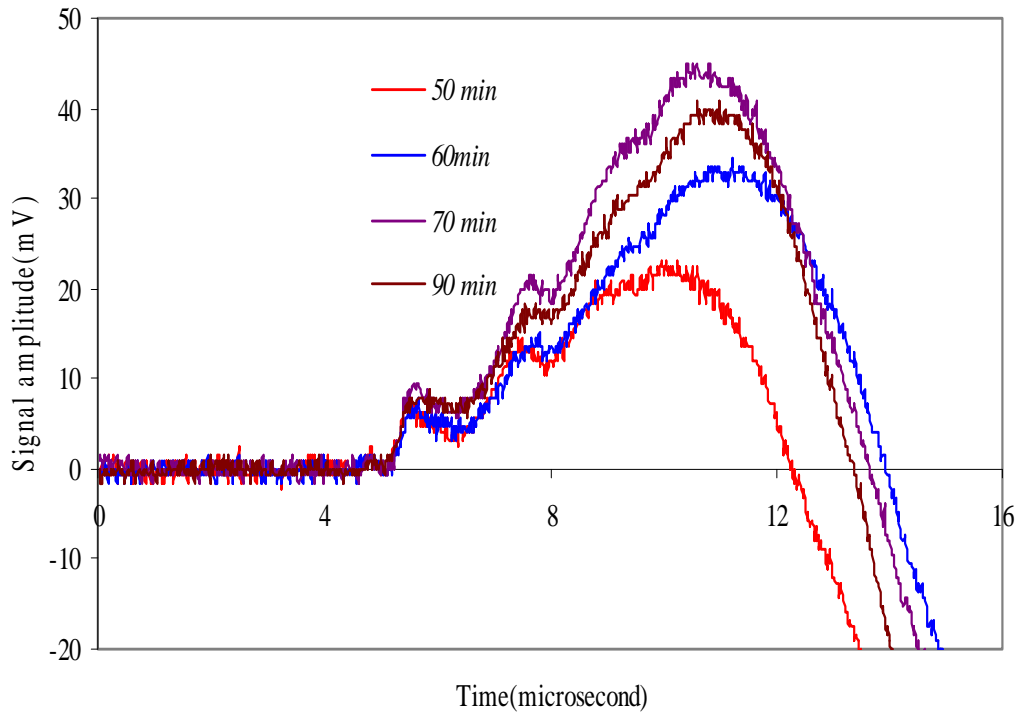


Figure 4.4 Interferometer waveforms for the arrival of an acoustic wave during the final stages of cure in a rapid cure room temperature epoxy of 1 mm thickness at room temperature. The signals were recorded 50, 60, 70 and 90 min after the epoxy was mixed with the curing agent.

4.3 Time delay measurement algorithm

Different approaches were attempted to determining the time for the onset ultrasonic pulse and finally an algorithm was developed using Excel software. The data points captured were transferred to the column B of the spread sheet as shown in figure 4.5. Then an 11-point moving average was calculated. For the calculated points again an 11-point moving average calculated and named as a “double moving average”. The maximum of the double moving average calculated and all three sets of data, original, moving average and double moving average points were normalised. Then 10-point moving gradient calculated and the raw data, double smoothed data and slope of doubly smoothed data were plotted as shown in figure 4.6. Then y-intercepts and x-intercepts were calculated and inferred X- intercepts were plotted as shown in figure 4.7. The maximum x-intercept calculated, after multiplying by the interferometric scaling factor, time corresponding to the maximum gradient was chosen as the onset ultrasonic arrival time.

	A	B	C	D	E	F	G	H	I	J	K
1	259.3	paste raw data here	Smoothed	Dbl smoothed	Norm Original	Norm smooth	Norm dblsm	Slope*100	Slope*100	Slope*100	y-intercept
2	Arrival point	first clear row 500...						norm orig	norm smth	norm dblsm	original
261	253	512	442.182	480.264	0.035	0.030	0.033	0.208	0.064	0.136	-0.497
262	254	256	512.000	488.727	0.018	0.035	0.034	0.144	0.083	0.204	-0.331
263	255	512	488.727	509.884	0.035	0.034	0.035	0.241	0.140	0.290	-0.580
264	256	0	535.273	543.736	0.000	0.037	0.037	0.064	0.242	0.400	-0.127
265	257	768	558.545	611.438	0.053	0.038	0.042	0.128	0.373	0.537	-0.291
266	258	768	512.000	696.066	0.053	0.035	0.048	0.112	0.532	0.702	-0.254
267	259	768	558.545	799.736	0.053	0.038	0.055	0.273	0.714	0.895	-0.668
268	260	512	698.182	924.562	0.035	0.048	0.064	0.545	0.946	1.113	-1.369
269	261	512	861.091	1091.702	0.035	0.059	0.075	0.978	1.222	1.347	-2.494
270	262	768	1140.364	1294.810	0.053	0.079	0.089	1.347	1.538	1.589	-3.450
271	263	256	1348.818	1538.116	0.018	0.093	0.106	1.812	1.869	1.831	-4.672
272	264	1024	1582.545	1836.430	0.071	0.109	0.127	2.213	2.190	2.061	-5.733
273	265	1792	1885.091	2174.942	0.123	0.130	0.150	2.694	2.475	2.271	-7.009
274	266	2304	2327.273	2540.959	0.159	0.160	0.175	3.271	2.719	2.445	-8.541
275	267	3072	2769.455	2930.248	0.212	0.191	0.202	3.544	2.902	2.574	-9.271
276	268	3072	3234.909	3325.884	0.212	0.223	0.229	3.768	3.032	2.648	-9.876
277	269	3328	3793.455	3732.099	0.229	0.261	0.257	3.640	3.070	2.663	-9.530
278	270	4096	4282.182	4146.777	0.282	0.295	0.286	3.415	3.017	2.621	-8.927
279	271	5376	4724.364	4555.107	0.370	0.326	0.314	3.223	2.866	2.526	-8.409
280	272	5376	5143.273	4933.818	0.370	0.354	0.340	2.999	2.636	2.384	-7.802
281	273	5888	5492.364	5285.025	0.406	0.378	0.364	2.774	2.354	2.203	-7.195
282	274	6400	5818.182	5602.380	0.441	0.401	0.386	2.229	2.035	1.991	-5.706
283	275	6400	6144.000	5875.306	0.441	0.423	0.405	1.636	1.729	1.759	-4.074
284	276	6656	6376.727	6105.917	0.459	0.439	0.421	1.026	1.426	1.522	-2.393
285	277	6912	6493.091	6304.793	0.476	0.447	0.434	0.738	1.159	1.292	-1.596
286	278	6912	6632.727	6465.587	0.476	0.457	0.445	0.449	0.913	1.078	-0.791
287	279	6656	6725.818	6596.760	0.459	0.463	0.455	0.257	0.694	0.885	-0.252
288	280	6912	6795.636	6702.545	0.476	0.468	0.462	0.273	0.522	0.719	-0.295
289	281	6656	6818.909	6780.826	0.459	0.470	0.467	0.080	0.407	0.578	0.245
290	282	6656	6912.000	6842.182	0.459	0.476	0.471	0.289	0.340	0.461	-0.338
291	283	6912	6912.000	6895.074	0.476	0.476	0.475	0.289	0.281	0.365	-0.341
292	284	6912	6935.273	6933.157	0.476	0.478	0.478	0.369	0.232	0.285	-0.570
293	285	7168	6981.818	6967.008	0.494	0.481	0.480	0.337	0.206	0.221	-0.479

Figure 4.5 first part of the excel algorithm screen shot.

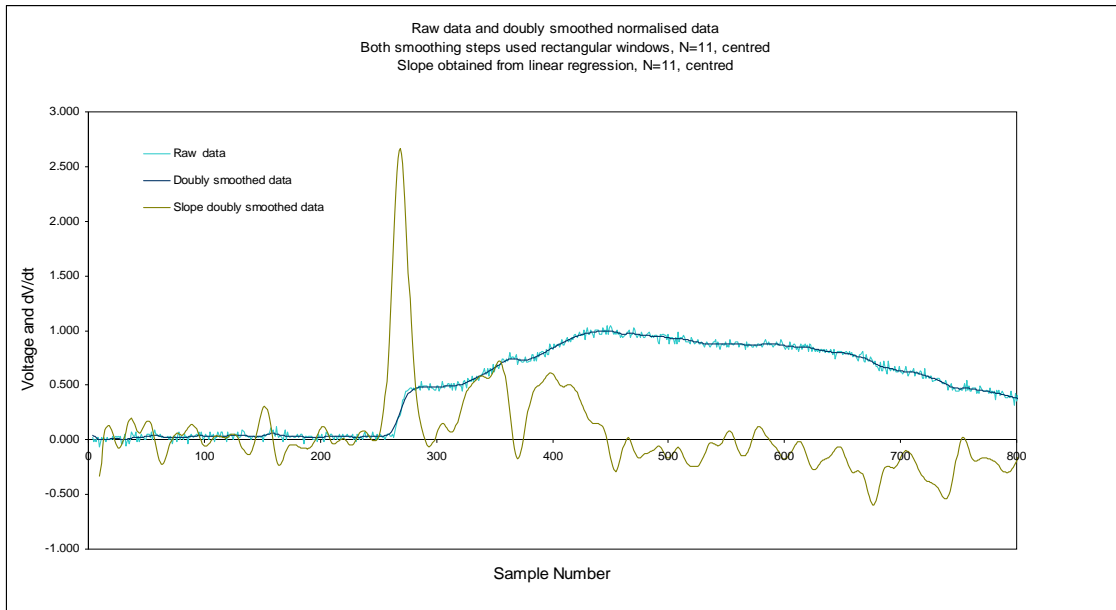


Figure 4.6 Raw data and doubly smoothed normalized data, both smoothing steps used rectangular windows, N=11, centred. Slope obtained from linear regression, N=11, centred.

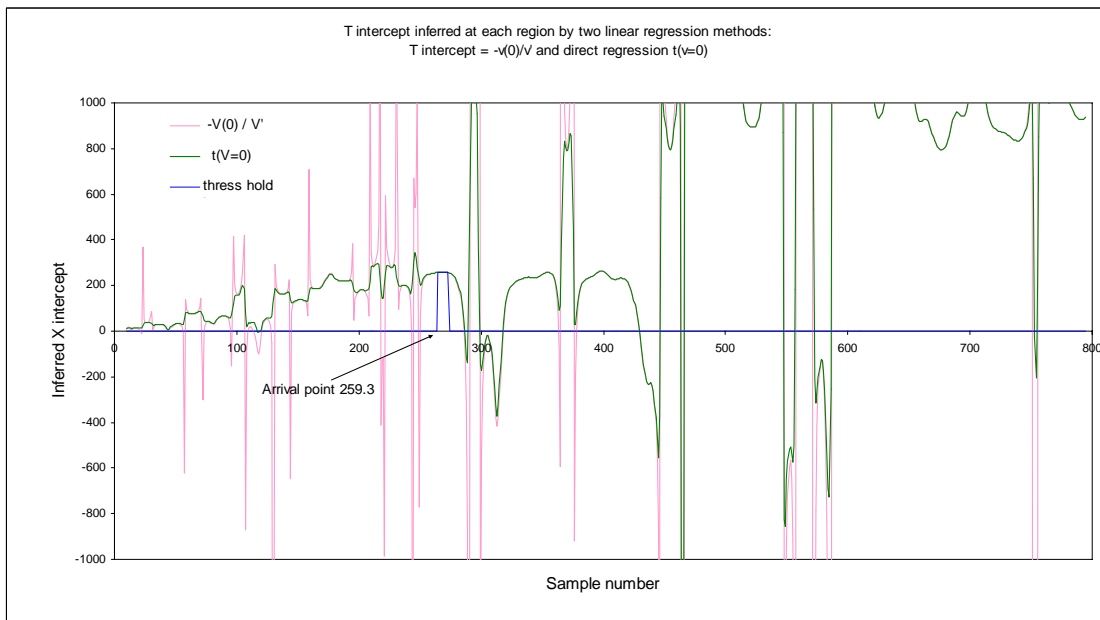


Figure 4.7 T intercept inferred at each region by two linear regression methods: T intercept = $-v(0)/v'$ and direct regression $t(v=0)$.

4.4 Variation of curing time with different thickness samples

The epoxy holder was adjusted to hold samples of thickness of 2, 4, 6, 10 and 12 mm and the interferometer waveforms were recorded for different curing times as shown in figures 4.8-4.13. Initially waveforms were recorded in 5 min intervals. As the cure progresses, the rate of change of the acoustic properties slows, allowing the interval between the measurements to increase to 10 and 20 min. The trend of the waveforms observed is consistent with previously reported works by Lindrose (1978), Hahn *et al.*, (1984), Ohn *et al.*, (1992) and Mitra *et al.*, (1999). The results above clearly indicate that this remote optical technique can be used to monitor the degree of cure. The time delay between the trigger pulse and the onset arrival of the first ultrasonic pulse is a measure of the cure state. Knowledge of the extent of the bonding reaction during the cure of a composite material is necessary to optimise the processing of these resins for commercial applications. This knowledge is essential for prevention of over cure or under cure. The rate at which the bond development progress depend on resin's chemical composition and temperature. Since typically these are not absolutely controllable, a monitor of the extent of cure provides important information useful for controlling the cure process. There are two basic parameters that can be measured with ultrasonic monitors: the time for the wave to transfer through the material (wave speed), and the energy absorbed by the material (attenuation). These parameters can be

related to the mechanical response of the materials. By monitoring the changes in wave speed and attenuation during cure, the cure state of the material can be assessed (Scott *et al.*, 1991).

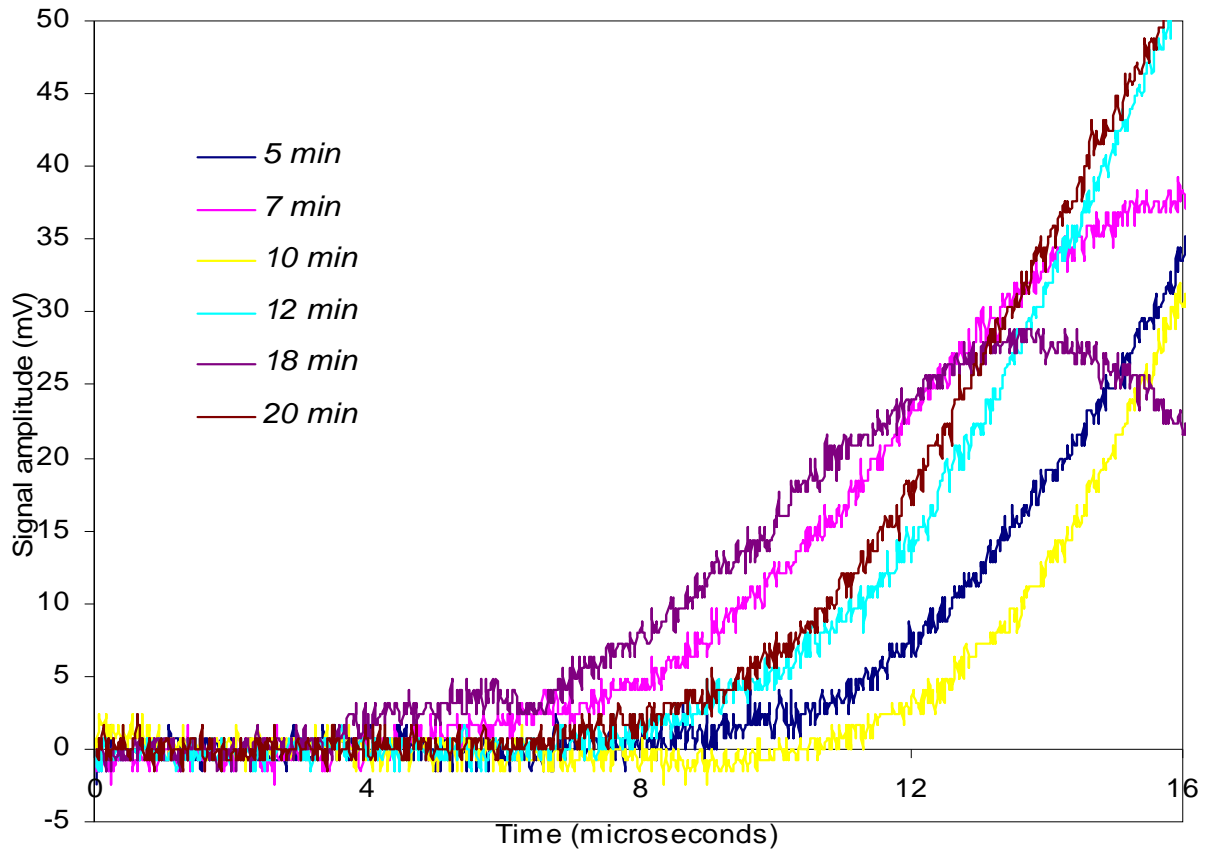


Figure 4.8 Interferometer waveforms for the arrival of an acoustic wave during the early stages of cure in a rapid cure room temperature epoxy of 2 mm thickness at room temperature. The signals were recorded 5, 7, 10, 12, 18 and 20 min after the epoxy was mixed with the curing agent.

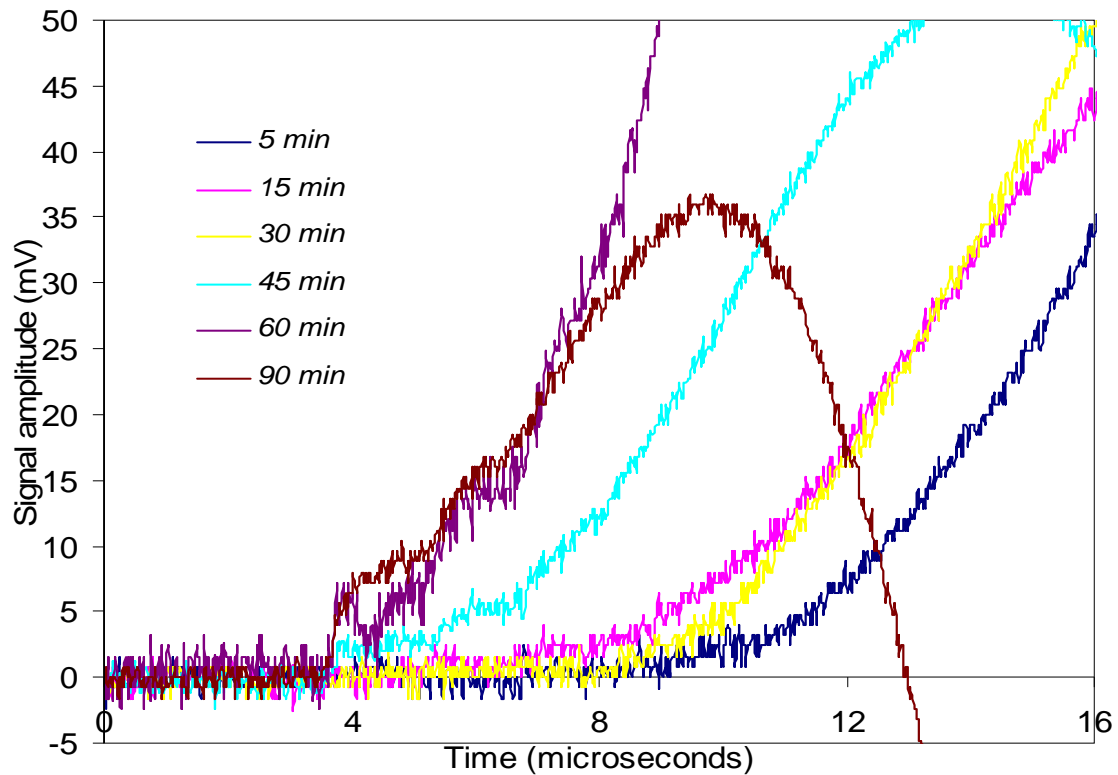


Figure 4.9 Interferometer waveforms for the arrival of an acoustic wave during different stages of cure in a rapid cure room temperature epoxy of 2 mm thickness at room temperature. The waveforms were recorded 5, 15, 30, 45, 60 and 90 min after the epoxy was mixed with the curing agent.

A sharp rising edge of the ultrasonic pulse is evident for the waveforms recorded after 15 min. The waveforms recorded for 60 min and 90 min have almost the same onset pulse arrival points.

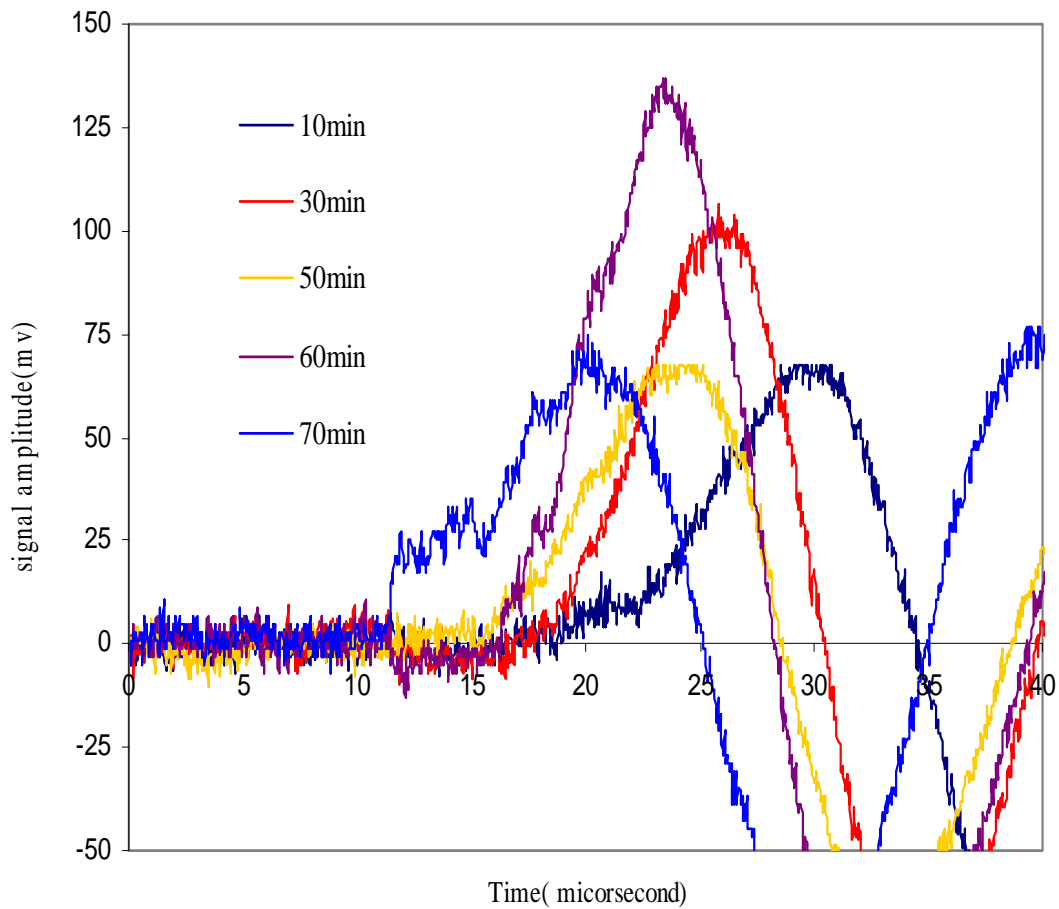


Figure 4.10 Interferometer waveforms for the arrival of acoustic wave during the early stages of cure in a rapid cure room temperature epoxy .The epoxy holder was adjusted to hold 4 mm thickness of the room temperature cure epoxy. The waveforms recorded for 10, 30, 50, 60 and 70 min after the epoxy was mixed with the curing agent were shown. The sharp rising edge of ultrasonic pulse is for the waveform recorded after 70 min is evident for the end of cure state.

A sharp rising edge of the ultrasonic pulse is evident for the waveforms recorded after 15 min. The waveforms recorded for 60 min and 90 min almost have the same onset pulse arrival points.

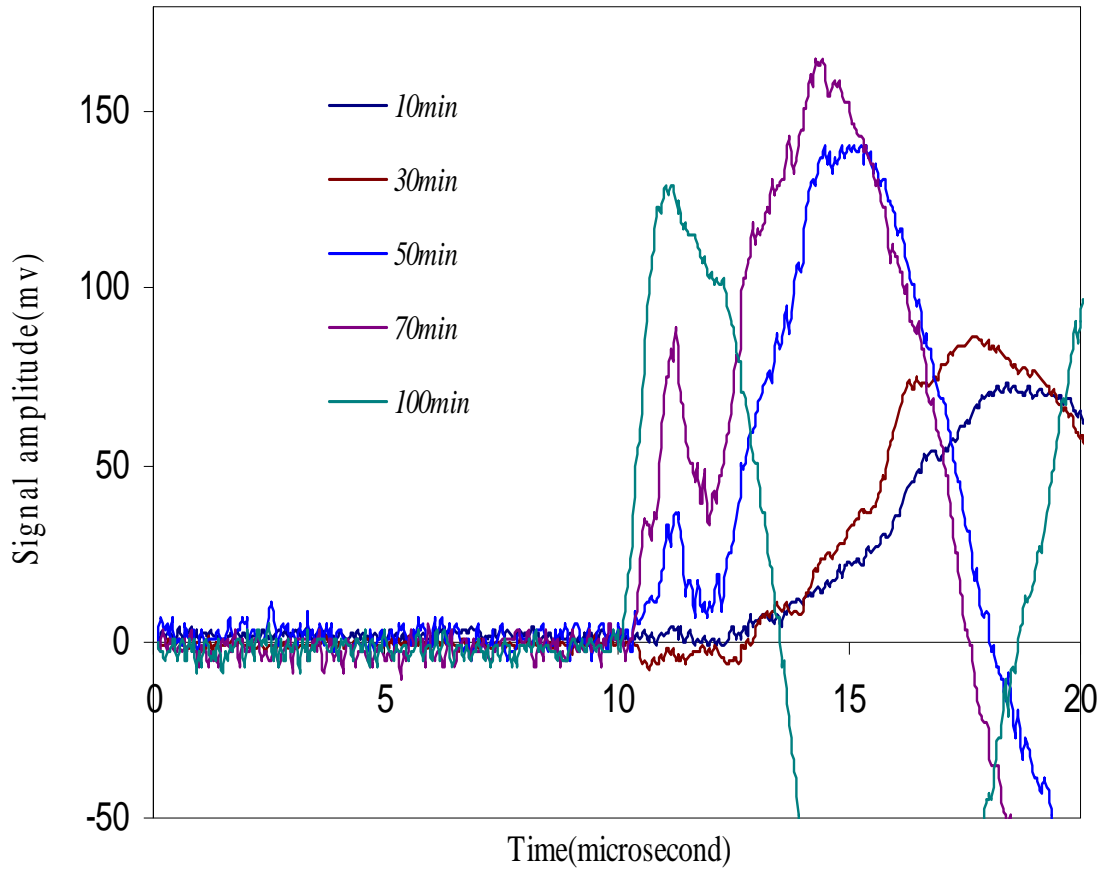


Figure 4.11 Interferometer waveforms for the arrival of an acoustic wave during the final stages of cure in a rapid cure room temperature epoxy of 6 mm thickness at room temperature. The waveforms recorded for 10, 30, 50, 70 and 100 min after the epoxy was mixed with the curing agent were shown.

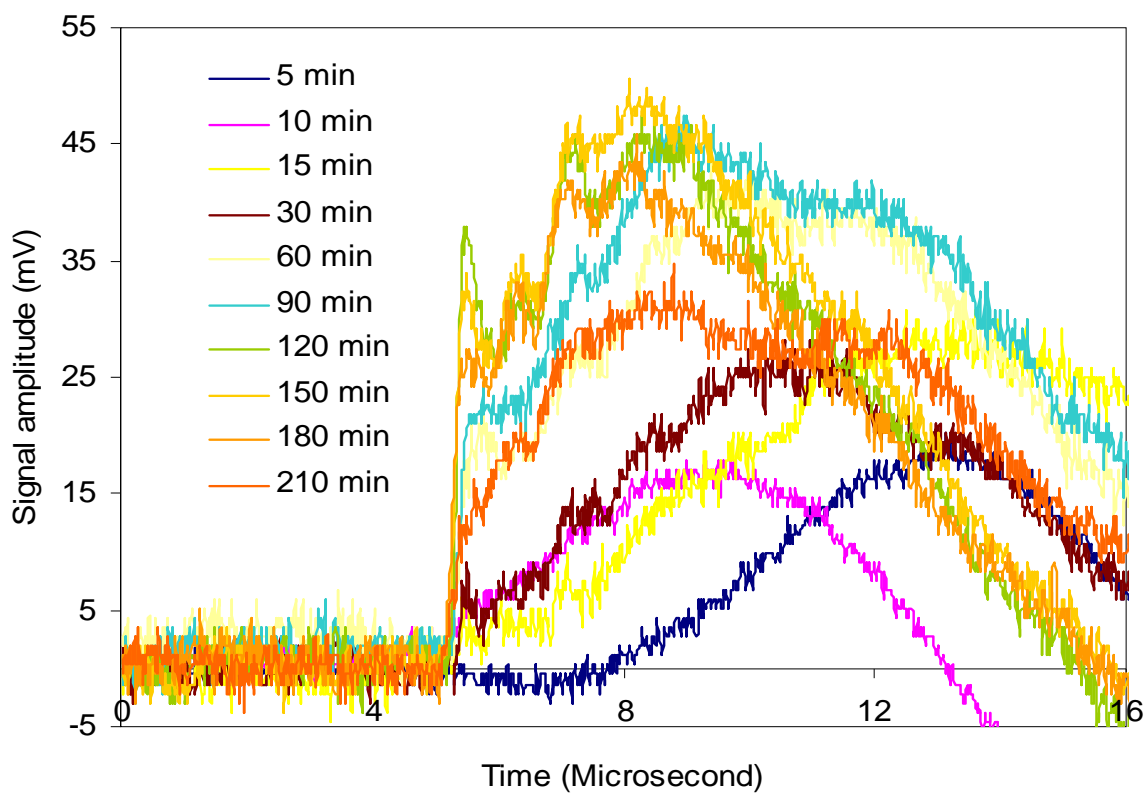


Figure 4.12 Interferometer waveforms for the arrival of an acoustic wave during the final stages of cure in a rapid cure room temperature epoxy of 10 mm thickness at room temperature.

A sharp rising edge of the ultrasonic pulse is first time evident for the waveform recorded for 30 min. The waveforms recorded after 30 min have a sharp onset pulse arrival points.

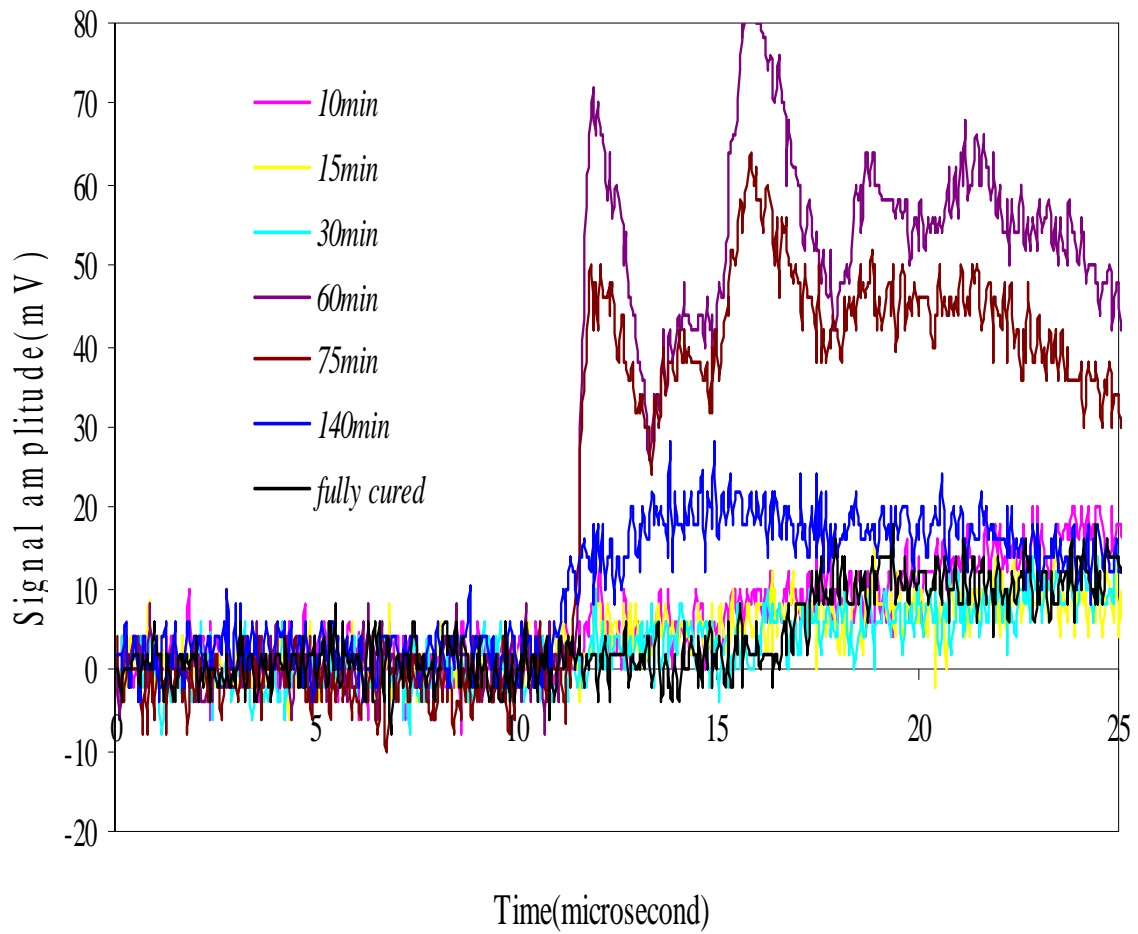


Figure 4.13 Interferometer waveforms for the arrival of an acoustic wave during the curing stages of room temperature epoxy. The epoxy holder was adjusted to hold 12 mm thickness of the epoxy.

The waveform recorded after 24 hours is entirely different to the trend observed it may be due to the lack of contact between the front end of the epoxy holder (Teflon material) and the completely cured sample.

4.5 Variation of time delay with thickness.

The onset arrival times for the pulse were calculated using the algorithm developed in section 4.3. The relative ultrasonic travel times for 1, 2 and 10 mm thickness of samples were calculated and plotted as shown in figures 4.14-4.16. The sharp decrease in the relative time delay, during the cure process could be attributed to the rapid increases in the degree of cure. The end of cure could be determined from the time when the relative travel time approaches zero. It should be noted that a number of researchers have measured a similar time delay during the cure of epoxy (Chen *et al.*, (1999), Ohn *et al.*, (1992) and Dorigi *et al.*, (1997). The gradual decreases of the time delay corresponding to the progressive cross linking reaction of the composite. The effect of the state of cure on the time delay can be, therefore, described as continuous decreases of the time delay as the material change from a liquid, through a gel, to a solid due to increasing moduli of the composite Chen *et al.*, (1999). The inferred cure time for different thickness of samples were shown in figure 4.17. The inferred cure time increases as thickness increases.

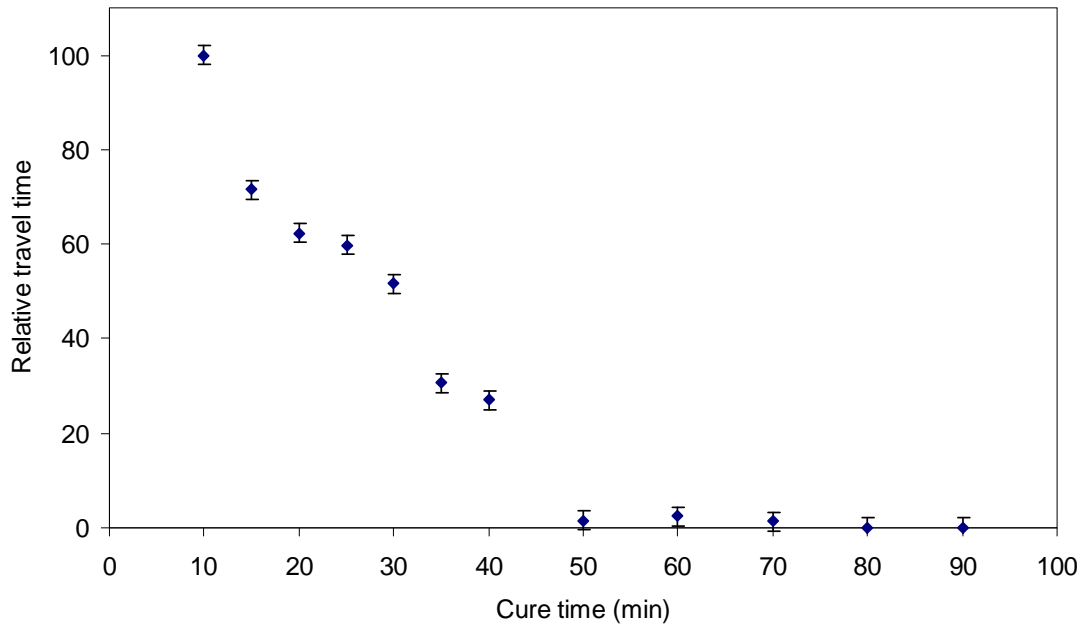


Figure 4.14 Relative travel time against the cure time for a 1 mm thickness sample.

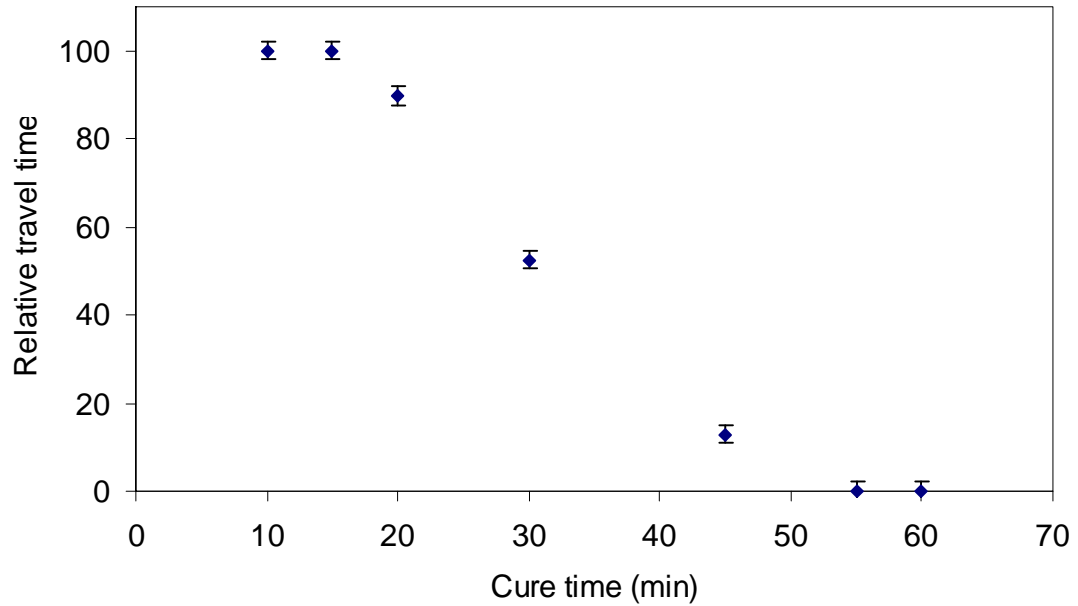


Figure 4.15 Relative travel time against the cure time for a 2 mm thickness sample.

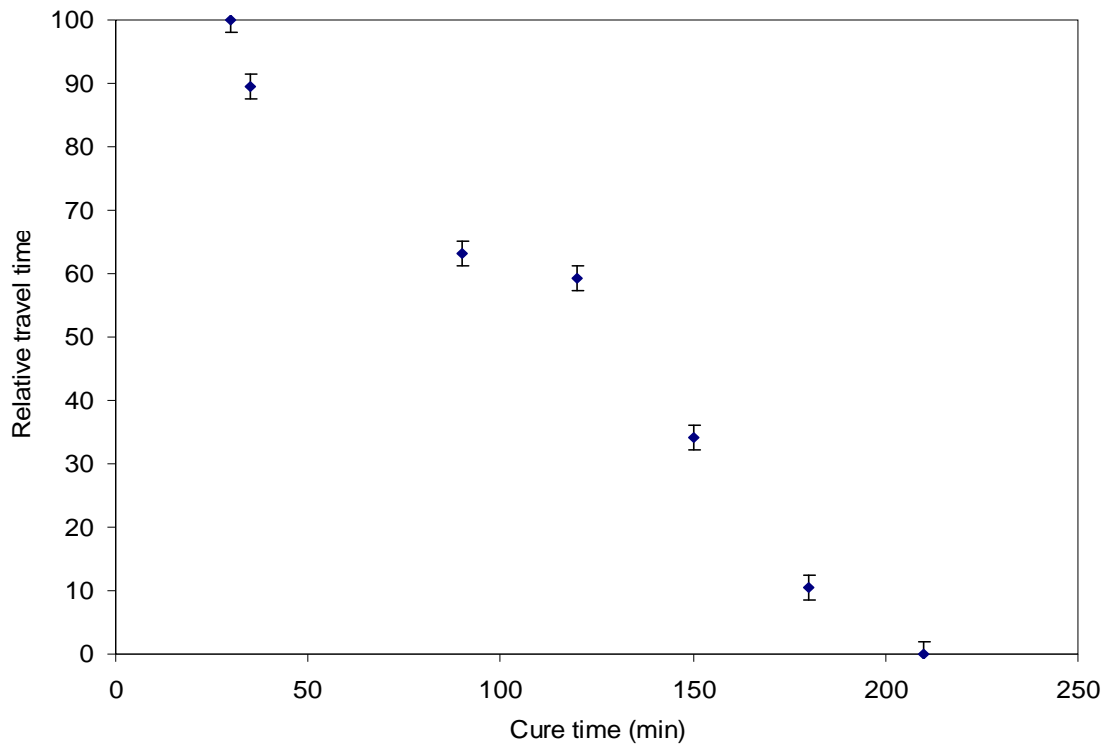


Figure 4.16 Relative travel time against the cure time for a 10 mm thickness sample.

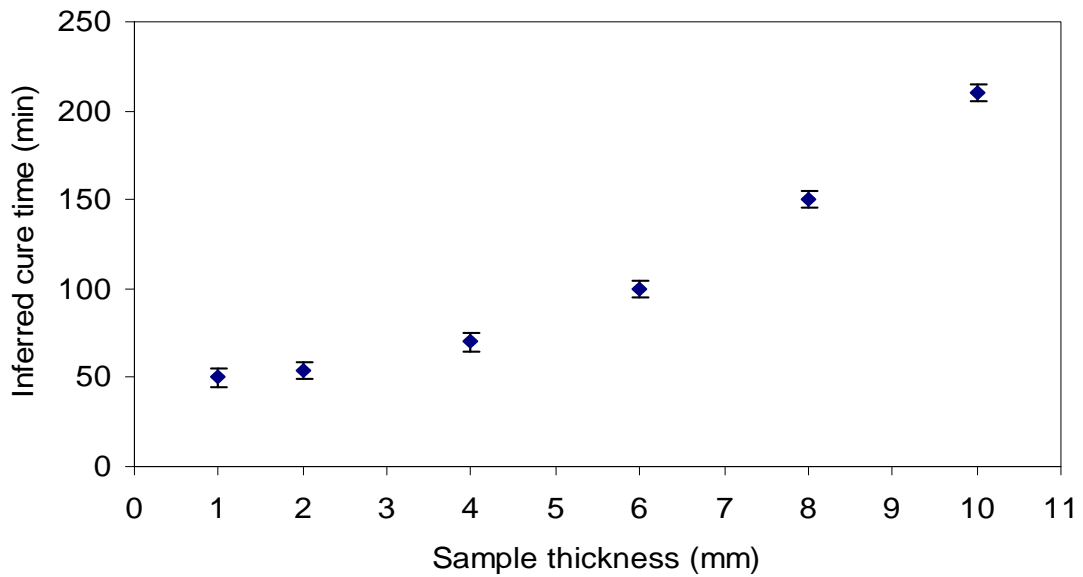


Figure 4.17 Inferred cure time against the sample thickness.

4.6 Variation of attenuation with thickness.

Ultrasonic attenuation measurements are widely used to characterize materials. Such measurements can be used to estimate various physical parameters such as grain size, tensile strength and yield strength. The relative attenuation of the signal is plotted in figure 4.18. This attenuation is defined in a manner similar to Hahn *et al.*, (1984) as $20\log (A/A_1)$ where A is the amplitude of the first longitudinal wave pulse and A₁ is the amplitude of that pulse for which the amplitude can be determined precisely.

The relative attenuation increases, but after reaching a peak, it drops down to a value lower than the initial value. This in agreement with the results of Hahn *et al.*, (1984) who used a quite different epoxy. The ultrasonic velocity and attenuation measured during the isothermal cure at room temperature (20°C) for different thickness of samples were reported in Figures 4.12 - 4.14. It is seen in these figures that the longitudinal velocity increase from an initial value to a final during the cure.

The ultrasonic attenuation of the epoxy for different thickness of samples is shown in Figure 4.17. Initially the attenuation started increasing and during the middle of the cure it had a peak value and again started decreasing. The peak of the ultrasonic attenuation result when the ultrasonic frequency used to interrogate the epoxy is the inverse of the relaxation time of the resin. The relaxation time of an epoxy resin increases during the process of polymerisation; this has been attributed to the increase in the length of the polymer chain during cure (Dorigi *et al.* 1997).

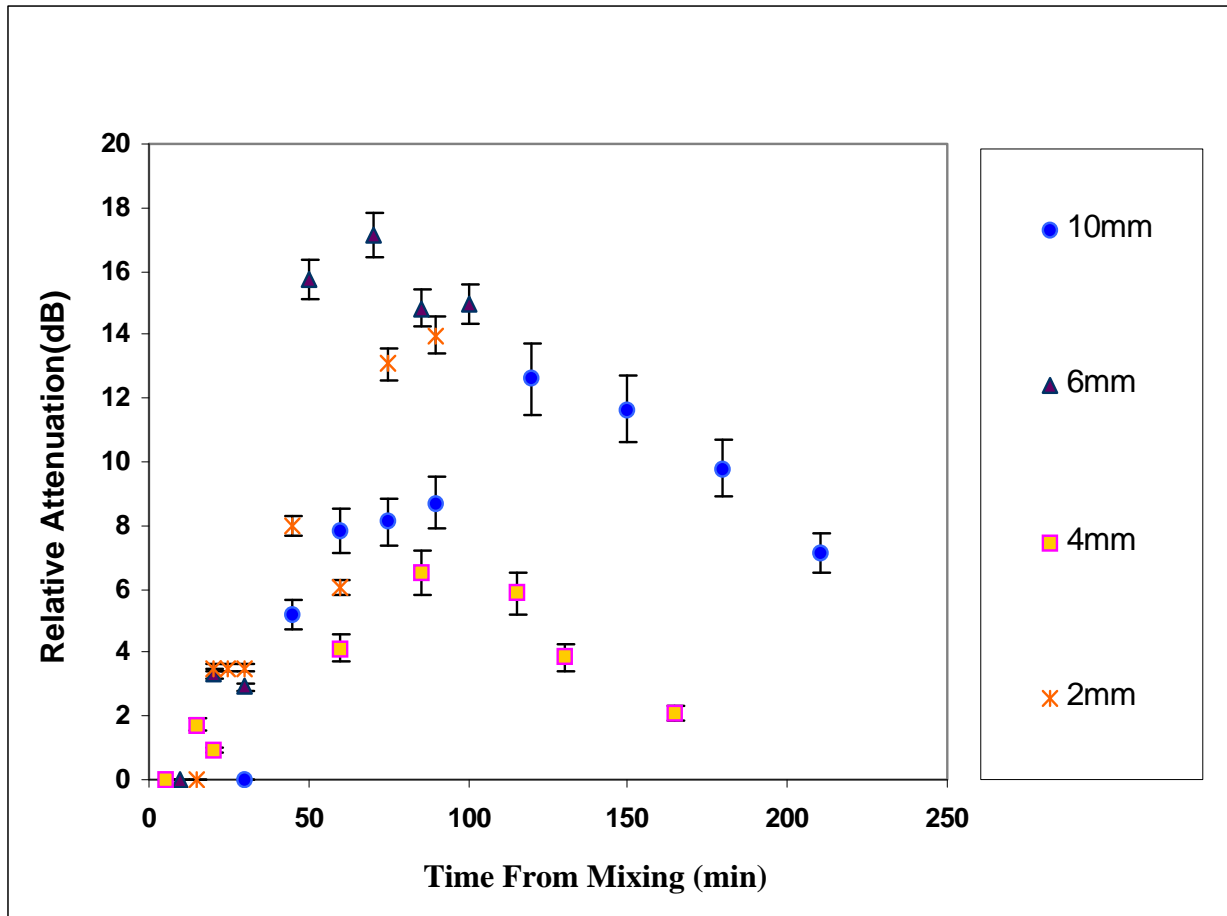


Figure 4.17 Relative attenuation against the time from mixing of the epoxy with the curing agent for samples with thickness 2, 4, 6 and 10 cm.

The ultrasonic attenuation goes through a maximum during the region where the most rapid changes in time delay occur. Then, the attenuation drops dramatically, indicating the rapid rise of viscosity due accelerated cross linking at that stage. Afterward, the attenuation gradually decreases because, as cross linking proceeds, the material behaves more like an elastic medium, which reduced absorption of ultrasonic energy (Chen, 1999).

4.7 Conclusion

The cure of epoxy resin has been successfully monitored using the described non contact optical technique. Both relative ultrasonic travel time and ultrasonic attenuation were monitored as the cure progresses. The variation of inferred cure time against different thicknesses of samples also reported. It should be noted that this is the first time the fully non-contact ultrasonic techniques were used to monitor the travel time and attenuation for different thicknesses epoxy samples.

Samples of thickness 1-12 mm were made and for each thickness, the experiment was repeated five or six times and observed that the waveforms are following a similar pattern as the cure progresses. For a particular thickness, the similar waveforms can be reproducible for different samples.

The non-contact optical technique has been shown to work satisfactorily for epoxy samples of thickness from 1 to 12 mm thickness. The silver paint on the front surface increases the interferometer signal amplitude and the power of the interferometer detection system need not be larger than 2 mW and would allow the system to be use in industrial environments.

Chapter 5

Conclusion

The aim of this research, the monitoring of the curing process of composite materials using non-contact optical techniques, has been achieved. Acoustic waves were generated in the curing materials through exposure to a Q-switched Nd:YAG laser with output energy of about 130 mJ, which was in the slight ablation regime. A sensitive wide-bandwidth optical fiber optic interferometer, which was constructed by Mitra (1996), was calibrated and used remotely to monitor the position of one surface and thereby to detect the acoustic waveforms.

A cylindrically-shaped epoxy holder was constructed to hold the liquid state epoxy. The material Teflon was chosen because of its special property of not sticking to the cured epoxy. To ensure that the laser pulses generated ultrasonic waves of sufficient amplitude in the epoxy samples, one side of the epoxy holder consisted of a copper strip. The other side was painted with silver paint to enable a good reflection for the interferometer beam back into the sensing fibre tip.

Samples of thicknesses 1-12 mm were made and, for each thickness, the waveforms were captured in 5 min intervals until a sample was fully cured. The procedure was repeated five or six times and it was observed that the waveforms were following a similar pattern as the cure progresses. The waveforms captured during the early stage, within 10 min from mixing with curing agents, look similar to each other and after that significant change to wave shapes were observed.

As the cure process started the mechanical properties of the epoxy changed significantly allowing faster ultrasonic propagation. The time interval between the trigger pulses to the onset of the rise of the acoustic pulse is the propagation time. Determining the exact

time of the arrival of the acoustic pulse was essential for determining the propagation time. The waveforms recorded at early stages of curing were significantly affected by the noise picked up from the electronic circuits. An algorithm was developed using Microsoft Excel to calculate the arrival time of the acoustic wave pulse in each experimental waveform.

It was evident from these results that the ultrasonic wave travel time decreases as the cure progresses. This was consistent with the findings of several researchers who used the ultrasonic waves travel time through the epoxy sample as a cure monitoring parameter. Importantly, though, this thesis has reported, for the first time, the use of a fully remote optical technique to both generate and monitor the acoustic waveform for different thicknesses of samples during their curing process. This is particularly useful, as the ultrasonic velocity (or the bulk longitudinal modulus) can be considered the most interesting parameter for cure monitoring because it follows the growth and evolution of the mechanical stiffness of the resin during cure (Maffezzoli, A, 1999).

The relative attenuation of ultrasonic waves was also investigated and used as another method for monitoring the curing process. The relative attenuation was calculated and plotted against curing time. In the results the relative attenuation increased, but, after reaching a peak, it decreases to a value lower than the initial value. This is in agreement with the results of Hahn *et al.* (1984) who used an entirely different type of epoxy with contact transducers to monitor acoustic waveforms.

Thus this all-optical remote excitation and detection system is capable of monitoring the curing process of epoxies. The work from this thesis has contributed to improved understanding of the cure of composite in materials of different thickness.

References

Achenbach J. D., "Ultrasonic Characterization of Thin Film Material Constants and Defects", *Key Engineering Materials*, Vol. 270-273, pp. 8-13, 2004.

Afromowitz M. A and Kai-Yuen L., "Optical properties of curing epoxies and applications to the fiber optic composite cure sensor", *Proc. SPIE, Fiber Optic Smart Structures and Skins II*, Vol. 1170, pp. 138-142, 1989.

Albert M. L., "Ultrasonic wave and moduli changes in a curing epoxy resin", *Experimental Mechanics*, Vol. 18, pp. 227-232, 1978.

Alderson K. L., Webber R. S., Mohammed U. F. and Murphy E., "An experimental study of ultrasonic attenuation in microporous Polyethylene", *Applied Acoustics*, Vol. 50, pp. 23-33, 1997.

Aussel J. D. and Monchalin J. P., "Precision laser-ultrasonic velocity measurement and elastic constant determination", *Ultrasonics*, Vol. 27, pp. 165-177, 1989.

Aussel J. D., Le Brun A. and Baboux J. C., "Generating acoustic waves by laser: Theoretical and experimental study of the emission source", *Ultrasonics*, Vol. 26, pp. 245-255, 1988.

Balasubraminiam K. and Whitney S. C., "Ultrasonic through-transmission characterization of thick fiber-reinforced composites, *NDT&E International*, Vol. 29, pp. 225-236, 1996.

Baldwina K. C., Berndtb T.P., Ehrlich M.J., "Narrow band laser generation/air-coupled detection: ultrasonic system for on-line process control of composites", *Ultrasonics*, Vol. 37, pp. 329-334, 1989.

References

Blouin A., Lévesqu D. E., Néron C., Drolet D. and Monchalin J. P., “Improved resolution and signal-to-noise ratio in laser-ultrasonics by SAFT processing”, *Optics Express*, Vol. 2, pp. 531- 539, 1998.

Buma T., Spisar M. and O'Donnell M., “High-frequency ultrasound array element using thermoelastic expansion in an elastomeric film”, *Applied Physics Letters*, Vol. 79, pp 548-550, 2001.

Burianova L., Kopal A. and Nosek J., “Characterization of advanced piezoelectric materials in the wide temperature range”, *Materials Science and Engineering*, Vol. 91, pp. 187-191, 2003.

Chehural E., Skordos A. A., Ye C. C., James S. W. and Partridge I. K., “Strain development in curing epoxy resin and glass fibre/epoxy composites monitored by fibre Bragg grating sensors in birefringent optical fibre”, *Smart Materials Structure*, Vol. 14 , pp. 354–362, 2005.

Chen J. Y., Hoa S. V., Jen C. K. and Wang H., “Fibre-optic and ultrasonic measurements for in-situ cure monitoring of graphite/epoxy composites”, *Journal of Composite Materials*, Vol. 33, pp. 1860-1881, 1999.

Chen J. Y., Johnaston A., Petrecue L. and Hojjati M., “A novel calorimetry technique for monitoring electron beam curing of polymer resin”, *Radiation Physics and Chemistry*, Vol. 25, pp. 336-349, 2006.

Chew S. and Sim A., “Monitoring partially-cured epoxy adhesive in disc-drive sub assembly by thermal analysis (TA) techniques”, *IEEE*, pp. 181-188, 5th International Physics Failure Analysis (IPFA'95), 1995.

References

Cordovez Y. L. M. and Karbhari V. M., “Dielectric and mechanical characterization of processing and moisture uptake effects in E-glass/epoxy composites”, *Composites*, Vol. 34 Part B, pp. 383–390, 2003.

Davis A., Ohn M. M., Liu K. and Measures R. M., “A study of an opto-ultrasonic technique for cure monitoring”, *Proc. SPIE*, Vol. 1588, pp. 264-274, 1991.

Daly J. H., Jeffrey K., Hayward D. and Pethritc R. A., “Use of thermally stimulated discharge measurements for the investigation of cure and characterisation of thermoset-epoxy resins systems”, *Journal of Material Science*, Vol. 28, pp. 2028-2034, 1993.

Dewhurst R. J. and Al’Rubai W. S. A. R., “Generation of short acoustic pulses from an energetic picosecond laser”, *Ultrasonics*, Vol. 27, pp. 262-269, 1989.

Dewhurst R. J., Nurse A. G. and Palmer S. B., “High power optical fibre delivery system for the laser generation of ultrasound”, *Ultrasonics*, Vol. 26, pp. 307-310, 1988.

Dewhurst R. J., Hutchins D. A., Palmer S. B. and Scruby C. B., “Quantitative measurements of laser-generated acoustic waveforms”, *Journal of Applied Physics*, Vol. 53, pp. 4064-4071, 1982.

Dombink K., Pieprzyca T., Sens J. and Wolf R., “Chemistry and materials science”, 1998, viewed 16 July 1999, <http://jchemed.chem.wisc.edu/ice/materials/composite.html>.

Dorighi J., Krishanaswamy S. and Achenbach J., “A fibre optic ultrasonic system to monitor the cure of epoxy”, *Research on Non-destructive Evaluation*, Vol. 9, pp. 13-24, 1997.

Ellis B., “Chemistry and Technology of Epoxy Resins”, Blackie Academic & Professional Press, Glasgow, UK, 1993.

References

Fomitchov P. A., Kromin A. K., Krishnaswamy S. and Achenbach J. D., “Imaging of damage in sandwich composite structures using a scanning laser source technique”, *Composites: Part B*, Vol. 35, pp. 557–562, 2004.

Fomitchov P. A., Krishnaswamy S. and Achenbach J. D., “Extrinsic and intrinsic fiber optic Sagnac ultrasound sensors”, *Optical Engineering*, Vol. 39, pp. 1972-1984, 2000.

Fromme P. and Sayri B. M., “Detection of cracks at rivet holes using guided waves”, *Ultrasonics*, Vol. 40, pp. 199-203, 2002.

George G. A., Cole-Clarke P., John N. S., and Friend G., “Real-time monitoring of the cure reaction of a TGDDM/DDS epoxy resin using fibre optics FT-IR”, *Journal of Applied Polymer Science*, Vol. 42, pp. 643-657, 1991.

Green R. E., “Non-contact ultrasonic techniques”, *Ultrasonics*, Vol. 42, pp. 9-16, 2004.

Hahn H.T., “Application of ultrasonic technique to cure characterization of epoxies”, *Non-destructive methods for material property determination*, edited by C.O Rudd and R.E. Green, pp. 315-326, Plenum Press, New York, 1984.

Hahn H. T., “Application of ultrasonic and thermal cure monitor of an epoxy resin”, *Proc. International SAMPE Symposium and Exhibition, Science of Advanced Materials and Process Engineering Series*, Vol. 36, pp. 284-297, 1991.

Hutchins D. A., Dewhurst R. J. and Palmer S.B. “Laser generated ultrasound at modified metal surfaces”, *Ultrasonics*, Vol. 19, pp. 103-108, 1981.

Imaino W. and Tam A. C., “Ultrasonic measurements in fine powders using a photoacoustic pulse-generation technique”, *Applied Optics*, Vol. 22, pp. 1875-1878, 1983.

References

Jang T. J., Lee S. S. and Kim Y. G., "Surface-bonded fiber optic Sagnac sensor for ultrasound detection", *Ultrasonics*, Vol. 42, pp. 831-842, 2004.

Kazilas M. C. and Partridge I. K., "Exploring equivalence of information from dielectric and calorimetric measurements of thermoset cure - a model for the relationship between curing temperature, degree of cure and electrical impedance", *Polymer*, Vol. 46, pp. 5868–5878, 2005.

Kersey A. D., Berkoff T. A., and Morey W.W., "Multiplexed fiber Bragg grating strain-sensor system with a Fabry-Perot wavelength filter", *Optics Letters*, Vol. 18, pp. 1370-1372, 1993.

Kim H. G. and Lee D. G., "Dielectric cure monitoring for glass/polyester prepreg composite", *Composite Structures*, Vol. 57, pp. 91-99, 2002.

Lam K. Y. and Afromowitz M. A., "Fibre optics epoxy composite cure sensor I. Dependence of refractive index of an autocatalytic reaction epoxy system at 850 nm on temperature and extent of cure", *Applied Optics*, Vol. 36, pp. 5635-5638, 1995.

Lam K. Y. and Afromowitz M. A., "Fibre optics epoxy composite cure sensor II. Performance characteristics", *Applied Optics*, Vol. 36, pp. 5639-5644, 1995.

Lee D. G. and Kim H. G., "Non-isothermal in situ dielectric cure monitoring for thermosetting matrix composite", *Journal of Composite Materials*, Vol. 38, pp. 977-993, 2004.

Leng G. and Asundi A., "Structural health monitoring of smart composite materials using EFPI and FBG sensors", *Sensors and Actuators*, Vol. 103, pp. 33-340, 2003.

References

Leng G. and Asundi A., “Real-time cure monitoring of smart composite materials using extrinsic Fabry–Perot interferometer and fibre Bragg grating sensors”, *Smart Materials and Structures*, pp. 249-255, 2002.

Liu Y. M., Ganesh C., Steele J. P. H and Jones J. E., “Fiber optic sensor development for real time in-situ epoxy cure monitoring”, *Journal of Composite Materials*, Vol. 31, pp. 87-102, 1997.

Maffezzoli A., Quarta E., Luprano V. A. M., Montagna G and Nicolais L., “Cure monitoring of epoxy matrices for composites by ultrasonic wave propagation”, *Journal of Applied Polymer Science*, Vol. 73, pp. 1969-1977, 1999.

Martian A. A and Kai-Yuen L., “Optical properties of curing epoxies and application to the fiber optic composite cure sensor”, *Proc. SPIE*, Vol 1170, pp. 138-142, *Fiber Optic Smart Structures and Skins II*, 1989.

McKie A. D. W. and Addison R. C., “Practical considerations for the rapid inspection of composite materials using laser-based ultrasound”, *Ultrasonics*, Vol. 32, pp. 333-345, 1994.

Mi B. and Ume C. I., “Parametric Studies of Laser Generated Ultrasonic Signals in Ablative Regime: Time and Frequency Domains”, *Journal of Nondestructive Evaluation*, Vol. 21, pp. 23-33, 2002.

Mitra B., “Remote detection of laser generated ultrasonics by fibre optic interferometer”, Ph.D. Thesis, Victoria University of Technology, 1997.

Mitra B. and Booth D. J., “Remote cure monitoring of epoxy materials using optical techniques”, *Ultrasonics*, Vol. 35, pp. 569-572, 1998.

References

Monchalain J. P., Nuron C. and Bussiure J. F., “Laser-ultrasonics: from the laboratory to the shop floor”, *Advanced Performance Materials*, Vol. 5, pp. 7–23, 1998.

Mozina J. and Hrovatin R., “Detection of excimer laser induced sub-picrometer ultrasonic displacement amplitudes”, *Ultrasonics*, Vol. 34, pp. 131-133, 1996.

Murukeshan V. M., Chan P. Y., Ong L. S. and Seah L. K., “Cure monitoring of smart composites using fiber Bragg grating based embedded sensors”, *Sensors and Actuators*, Vol. 79, pp. 153-161, 2000.

Nagel, D.J. and Imam M.A, “Energetics Of Defects And Strains In Palladium”, Tenth International Conference on Cold Fusion. 2003. Cambridge, MA: LENR-CANR.org.

Nakano T., Makishima S., Inoue Y. and Goto K., “Application of dielectric and thermal analysis to the curing of epoxy resins”, 7th International Conference on Dielectric Materials Measurements & Applications, pp. 23-26, 1996.

O’Dwyer M. J., Maistros G. M., James S. W., Tatam R. P. and Partridge I. K., “Relating the state of cure to the real-time internal strain development in acuring composite using in-fibre Bragg gratings and dielectric sensors”, *Measurement Science and Technology*, Vol. 9, pp. 1153–1158, 1998.

Ohn M. M., Davis A., Lis K. and Measures R. M., “Embedded fibre optic detection of ultrasound and its application to cure monitoring”, *Proc SPIE*, Vol. 1798. pp. 134-143, 1992.

Park J. M., Kong J. W., Kim D. S and Lee J. R., “Non destructive damage sensing and cure monitoring of carbon fibre/epoxyacrylate composite with UV and thermal curing using electro-micromechanical technique”, *Composite Science and Technology*, Vol. 64, pp. 2565-2575, 2004.

References

Park J. M., Lee S. I., and Choi J. H., "Cure monitoring and residual stress sensing of single-carbon fibre reinforce epoxy using electrical resistivity measurements", *Composite Science and Technology*, Vol. 65, pp. 571-580, 2005.

Papadakis E. P., "Monitoring the moduli of polymers with ultrasound", *Journal of Applied Physics*, Vol. 45, pp. 1218-1222, 1974.

Rath M., Doring J., Stark W. and Hinrichsen G., "Process monitoring of moulding compounds by ultrasonic measurements in a compression mould", *NDT&E International*, Vol. 33, pp. 123-130, 2000.

Rokhlin S. I., Lewis D. K., Graff K. F and Adier L., "Real-time study of frequency dependency of attenuation and velocity of ultrasonic wave during the curing reaction of epoxy resin", *Journal of Acoustic. Society of America*, Vol. 79, pp. 1786-1792, 1986.

Scruby C. B., "Some applications of laser ultrasonics", *Ultrasonics*, Vol. 27, pp. 195-209, 1989.

Scruby C. B. and Moss B. C., "Non-contact ultrasonic measurements on steel at elevated temperatures", *NDT&E International*, Vol. 26, pp. 177-188, 1993.

Scruby C. B., Dewhurst R. J., Hutchins D. A., and Palmer S. B., "Quantitative studies of thermally generated elastic wave in laser-irradiated metals", *Journal of Applied Physics*, Vol. 51, pp. 6210-6216, 1980.

Scott R. W. and Patrick T.M., "Ultrasonic and thermal cure monitor of an epoxy resin", 36th International SAMPE symposium, April 15-18, 1991.

References

Speake J. H., Arridge R. G. C. and Curtis G. J., "Measurement of the cure of resins by the ultrasonics techniques", *Journal of Applied Physics*, Vol. 7, pp. 412-424, 1974.

Spencer C. and Andrew S., "Monitoring Partially-cured Epoxy Adhesives in disc drive sub assembly by Thermal Analysis (TA) techniques", *IEEE*, pp. 181-188, 5th International Physics Failure Analysis (IPFA'95), 1995.

Sharama S. K., Schone C., L. and Cooney T. F., "Fibre-Optic remote Raman probe design for use in monitoring processes in a high temperature oven", *Applied Spectroscopy*, Vol. 47, pp. 377-379, 1993.

Shukal A., Letcher S., Brown C. and Rand G., "On the application of fibre optic sensors in physical, chemical and biological problems", *Experiments in Smart Materials and Structures (ASME)*, pp. 11-26, 1993.

Schmachtenberg E., Heide S. J. and Topker J., "Application of ultrasonics for the process control of Resin Transfer Moulding (RTM)", *Polymer Testing*, Vol. 24, pp. 330-338, 2005.

Thomas G.G., Toseph A. B., Anthony D., Sigel G. H., James H. C., Scott C.R and Richard G. P., "Optical fibre sensor Technology", *IEEE Journal of Quantum Electronics*, Vol. QE18, 1982.

Toussaint A., Cuypers P. and D'Hont L., "DSC and DMA Analysis of the curing of liquid Epoxy resin with diamines", *Journal of Coating Technology*, Vol. 57, pp. 71-82, 1985.

Ton-That M. T., Cole K. C., Jen C. K. and Franca D.R., "Polyester cure monitoring by means of different techniques", *Polymer Composites*, Vol. 21, pp. 605-618, 2000.

Vogt T., Lowe M. and Cawley P., "Cure monitoring using ultrasonic guided waves in wires", *Journal of Acoustic Society of America*, Vol. 114, pp. 1303- 1313, 2003.

References

Wanger J. W., Deaton J. B. and Spicer B., "Generation of ultrasound by repetitively Q-switching a pulsed Nd: YAG laser", *Applied Optics*, Vol. 27, pp. 4696-4700, 1988.

White, R. M., "Generation of elastic waves by transient surface heating", *J. Applied Phys.*, Vol. 34, pp. 3559-3567, 1963.

White S. R. and Kim Y. K., "Staged curing of composite materials", *Composites Part A*, Vol. 27A, pp. 219-227, 1996.

Whitney T. M and Green R., E., "Cure monitoring of carbon epoxy composites: an application of resonant ultrasound spectroscopy", *Ultrasonics*, Vol. 34, pp. 347-353, 1996.

Whitney T. M and Green R., E., "Nondestructive characterization of cure enhancement by high power ultrasound of carbon epoxy composite", *Material Science Forum*, Vol. 210-213, pp. 695-702, 1996.

Whitney T. M. and Green R. E., "Cure monitoring of carbon epoxy composites: an application of resonant ultrasound spectroscopy", *Ultrasonics*, Vol. 34, pp. 347-353, 1996.

Winfrey W. P. and Parker F. R., "Measurement of degree of epoxy cure with ultrasonic velocity", *IEEE 1984 Ultrasonics Symposium*, pp. 447-449, 1984.

Wu T. T. and Chen Y. C., "Dispersion of laser generated surface waves in an epoxy-bounded layered medium", *Ultrasonics*, Vol. 34, pp. 793-799, 1996.

Publications

- (1) S. Sathiyakumar and S. Collins, “Non contact monitoring of composite materials using Laser induced ultrasonic and fiber optic interferometer”, Australian Optical Society Conference, Sydney, Australia, 1999, Abstracts 36.

- (2) S. Sathiyakumar and S. Collins, “Cure monitoring of composite materials using optical techniques”, School of Communications and Informatics Research Forum SCIRF'99, Victoria University, Melbourne, Australia.

- (3) S. Sathiyakumar, S. Collins and A. Stevenson, “An experimental study of laser induced ultrasonic attenuation in composite materials using optical techniques”, Australian Optical Society Conference, Adelaide, Australia, 2000.